Article

Vegetation burning in the year 2000: Global burned area estimates from SPOT VEGETATION data

TANSEY, Kevin, *et al*.

Abstract

The scientific community interested in atmospheric chemistry, gas emissions from vegetation fires, and carbon cycling is currently demanding information on the extent and timing of biomass burning at the global scale. In fact, the area and type of vegetation that is burned on a monthly or annual basis are two of the parameters that provide the greatest uncertainty in the calculation of gas and aerosol emissions and burned biomass. To address this need, an inventory of burned areas at monthly time periods for the year 2000 at a resolution of 1 km2 has been produced using satellite data and has been made freely available to the scientific community. In this paper, estimates of burned area and number of burn scars for four broad vegetation classes and reported at the country level for the year 2000 are presented using data taken from the inventory. Over 3.5 million km2 of burned areas were detected in the year 2000, of which approximately 80% occurred in areas described as woodlands and shrublands. Approximately 17% of the burned area occurred in grasslands and croplands, the remaining 3% occurred in forests. Almost 600,000 [...]

Reference

TANSEY, Kevin, *et al*. Vegetation burning in the year 2000: Global burned area estimates from SPOT VEGETATION data. *Journal of geophysical research*, 2004, vol. 109, no. D14

DOI : 10.1029/2003JD003598

Vegetation burning in the year 2000: Global burned area estimates from SPOT VEGETATION data

Kevin Tansey,[1] Jean-Marie Grégoire,[2] Daniela Stroppiana,[3] Adélia Sousa,[4] João Silva,[5] José M. C. Pereira,[6,7] Luigi Boschetti,[2] Marta Maggi,[2] Pietro Alessandro Brivio,[3] Robert Fraser,[8] Stéphane Flasse,[9] Dmitry Ershov,[10] Elisabetta Binaghi,[11] Dean Graetz,[12] and Pascal Peduzzi[13]

Received 14 March 2003; revised 20 October 2003; accepted 29 October 2004; published 8 June 2004.

[1] The scientific community interested in atmospheric chemistry, gas emissions from vegetation fires, and carbon cycling is currently demanding information on the extent and timing of biomass burning at the global scale. In fact, the area and type of vegetation that is burned on a monthly or annual basis are two of the parameters that provide the greatest uncertainty in the calculation of gas and aerosol emissions and burned biomass. To address this need, an inventory of burned areas at monthly time periods for the year 2000 at a resolution of 1 km^2 has been produced using satellite data and has been made freely available to the scientific community. In this paper, estimates of burned area and number of burn scars for four broad vegetation classes and reported at the country level for the year 2000 are presented using data taken from the inventory. Over 3.5 million km^2 of burned areas were detected in the year 2000, of which approximately 80% occurred in areas described as woodlands and shrublands. Approximately 17% of the burned area occurred in grasslands and croplands, the remaining 3% occurred in forests. Almost 600,000 separate burn scars were detected. Descriptions of vegetation burning activity are given for ten regions. Finally, monthly burned area estimates are presented for the Central African Republic to illustrate the usefulness of these data for understanding, monitoring and managing vegetation burning activities. *INDEX TERMS:* 0305 Atmospheric Composition and Structure: Aerosols and particles (0345, 4801); 0315 Atmospheric Composition and Structure: Biosphere/atmosphere interactions; 1615 Global Change: Biogeochemical processes (4805); 1640 Global Change: Remote sensing; *KEYWORDS:* atmospheric chemistry, biomass burning, remote sensing

Citation: Tansey, K., et al. (2004), Vegetation burning in the year 2000: Global burned area estimates from SPOT VEGETATION data, *J. Geophys. Res.*, *109*, D14S03, doi:10.1029/2003JD003598.

1. Introduction

[2] Biomass burning is an annually occurring phenomenon affecting almost every vegetated ecosystem on Earth. Biomass burning is an important driver for global change owing to its effect on atmospheric composition and chemistry, climate, biogeochemical cycling of nitrogen and carbon, the hydrological cycle, the production of acid rain, the production of atmospheric black carbon that influences the absorption of sunlight, reflectivity and emissivity of land, and stability of ecosystems [*Levine*, 1996; *Levine et al.*, 1991; *Kaufman et al.*, 2002; *Govaerts et al.*, 2002]. One of the main uncertainties in the modeling of the climatic impact of aerosols is our knowledge of gas and aerosol emissions. To fully understand the impact of vegetation fires on the emissions of trace gases and aerosols and ecosystem functioning and cycling, information on the temporal and spatial distribution of burning activity and the type of vegetation burned is required at the global scale [*Van Aardenne et al.*, 2001; *Malingreau and Grégoire*, 1996; *Mack et al.*, 1996; *Andreae et al.*, 1996; *Dwyer et al.*, 1999]. In fact, the area consumed by fire at regional or global scales is one of the parameters that provides the greatest uncertainty in calculating the amount of burned biomass and emitted gases at this scale [*Scholes et al.*, 1996a; *Barbosa et al.*, 1999; *Andreae and Merlet*, 2001; *Levine*, 1996; *Isaev et*

[1]Department of Geography, University of Leicester, Leicester, UK.
[2]European Commission Joint Research Centre, Ispra, Italy.
[3]Institute for Electromagnetic Sensing of the Environment, Milan, Italy.
[4]Department of Rural Engineering, University of Évora, Évora, Portugal.
[5]Department of Forestry, Technical University of Lisbon, Lisbon, Portugal.
[6]Tropical Research Institute, Lisbon, Portugal.
[7]Also at Department of Forestry, Technical University of Lisbon, Lisbon, Portugal.
[8]Natural Resources Canada, Canada Center for Remote Sensing, Ottawa, Ontario, Canada.
[9]Flasse Consulting, Maidstone, UK.
[10]International Forest Institute, Moscow, Russia.
[11]Università dell'Insubria, Varese, Italy.
[12]CSIRO Earth Observation Centre, Canberra, ACT, Australia.
[13]United Nations Environment Programme, Geneva, Switzerland.

0148-0227/04/2003JD003598$09.00

al., 2002; *Taylor and Zimmerman*, 1991; *Conard et al.*, 2002]. There are existing data gaps and large differences in biomass burning and emission inventories, such as the Emission Database for Global Atmospheric Research (EDGAR) [*Olivier and Berdowski*, 2001] and the Global Emissions Inventory Activity (GEIA) [*Liousse et al.*, 1996], used for atmospheric chemistry modeling purposes. Recent campaigns including the Southern Africa Fire-Atmosphere Research Initiative (SAFARI) experiment (http://safari.gecp.virginia.edu/), the Experiment for Regional Sources and Sinks of Oxidants (EXPRESSO) experiment (http://www.ncar.ucar.edu/info/GTCP/expresso.html), the Biomass Burning Experiment: Impact on the Atmosphere and Biosphere (BIBEX) project (http://diotima.mpch-mainz.mpg.de/~bibex/Welcome.html) and the Large-Scale Biosphere-Atmosphere Experiment in Amazonia (LBA) project (http://lba.cptec.inpe.br/lba/indexi.html) have improved the characterization of emission factors and combustion characteristics a considerable amount and have allowed the computation of emission factors for many gas species [*Andreae and Merlet*, 2001]. However, much is unknown about the amount of biomass consumed by fire at large scales on an annual basis. Previous estimations have been largely based on regional data and extrapolation. Other estimates have relied on national statistics provided by countries without sufficient resources to derive accurate figures. The use of satellite data to derive information about the vegetation type and the burned area is one of many options available to the scientific community.

[3] The amount of biomass consumed by fire is related to the vegetation type, specifically the amount and composition of the fuel, and also the efficiency of the burning process. Not all biomass is available for burning, and it is important to adequately characterize the biomass that is available for burning. Specifically, the following factors influence the combustion of the vegetation: flammability (some plants contain oils), phenology (proportions of living and dead material), vegetation structure and the location of the fuel within the vegetation, weather conditions (humidity, wind speed, temperature), and fuel moisture levels. All of these factors influence the fire duration and intensity and consequently affect flaming and smoldering phases of burning activity. A high combustion rate will have an impact on the injection of gases higher into the atmosphere caused by the intense release of heat and the types and amounts of gases released under different fire conditions is also influenced by combustion. An overview of the trace gas emission estimations from biomass burning is given by *Palacios et al.* [2002]. While our knowledge is improving on understanding some of the factors described above and satellite-based studies are beginning to provide information on fire intensity and vegetation distribution, it is still lacking in one of the first numbers required for the estimation of burned biomass (BB) according to the equation by *Seiler and Crutzen* [1980]:

$$\mathrm{BB} = A \times D \times \alpha \times \beta, \tag{1}$$

where A is the area burned, D is the biomass density, α is the fraction of aboveground biomass, and β is the burning efficiency. In this paper, estimates for A are provided for the global scale at the resolution of 1 km^2. Recent estimates state that approximately 90% of the biomass burned in Africa originates from savanna fires, in contrast to South America and southeast Asia, where forest fires play a more significant role [*Delmas et al.*, 1991], and at the global scale, burning of African savannas is believed to account for almost one third of annual gross emissions from biomass burning [*Andreae*, 1997]. However, these estimates still suffer from significant levels of uncertainty, namely regarding the extent of area burned. In certain African countries, such as Sudan, Namibia, Angola, Madagascar, and Ethiopia, annual estimates of burned area at the country level are unknown, and only suggestions have been made owing to the difficulties in obtaining independent assessments of burning activity (for more information, refer to http://www.fire.uni-freiburg.de/iffn/country/country.htm).

[4] It is important to know the timing of burning activity for a number of reasons. For example, in the African savanna, burning during the early part of the dry season, when the vegetation cover is still wet, reduces the combustion completeness and the combustion efficiency compared to burning toward the end of the dry season [*Hoffa et al.*, 1999]. The emissions during the flaming and smoldering phases may also be different, and from the point of view of the land managers, fire timing plays an important role in controlling the characteristics of the succession vegetation.

[5] Short-term cycling of carbon occurs in the tropical savanna regions as the vegetation grows on an annual basis. For stand-replacing, forest fires where the burned biomass may take from decades to centuries to regrow, or where fire is used to convert land cover types such as forest to cropland, the prefire carbon pool of the forest becomes permanently transferred to the atmosphere. Stand-replacing fires are occurring in tropical forests, and emissions from these fires are believed to be making a substantial contribution to global warming through land conversion in Brazil [*Fearnside*, 2000]. They are also occurring in boreal forests where fire is both a widespread and an important factor and under current projections of climate warming will increase in frequency and severity and up to one quarter of the carbon stored in boreal forests could be lost to the atmosphere under changing climate scenarios [*Kasischke et al.*, 1995]. Isolated devastating fires such as those that occurred in Indonesia in 1997 released huge amounts of carbon into the atmosphere because large reservoirs of carbon stored in peat and natural forests were consumed with massive impacts on air quality, health, and atmospheric CO_2 concentrations [*Page et al.*, 2002].

[6] To address this need for better quantification of the burned area extent and timing, and to provide the scientific community with a reliable and well-documented data set, an inventory of burned areas at a resolution of 1 km for broad vegetation types including broadleaf forests, needleleaf and mixed forests, woodlands and shrublands and grasslands, and croplands has been produced. Broad vegetation types have been selected to present the findings in a clear and consistent manner, without using regional vegetation types or local names for vegetation. However, the full resolution data set is available to the scientific community to derive estimates of burned area per regional vegetation types. The

inventory, available in monthly time periods, was derived from satellite data acquired on a daily basis during the year 2000. Monthly burned area estimates for different vegetation types are presented for the Central African Republic (CAR) in Africa to illustrate the usefulness of monthly information contained in the inventory. Although data are available at the global scale, it is an exhaustive task to present monthly burned area estimates for all countries in this paper. The products described in this paper have been produced using fully documented methods under the Global Burned Area 2000 (GBA-2000) initiative [*Tansey*, 2002] and make a large contribution to the scientific understanding of the timing, extent, and location of burning activity at the global scale.

[7] The estimates of burned areas in this paper have the distinct advantage in that they are produced from a single source of information, namely satellite data from the VEGETATION (VGT) sensor aboard the European SPOT-4 satellite. Previous estimates of burned areas at the global scale have been derived from compilations of regional-scale studies and a best guess made in remote regions or those not directly specified in the literature. In addition, estimates often come from many different sources, use complicated methods, or are badly documented. Large variations in published values make the user communities reluctant to utilize the data available to them. To highlight this point, five estimates from four published articles of the annual burned area (both from multiannual year averages or single year estimates) in Russian forests ranged between 1.2 and 15 million hectares [*Food and Agricultural Organization of the United Nations* (*FAO*), 2001; *Stocks*, 1991; *Lavoué et al.*, 2000; *Shvidenko and Goldammer*, 2001]. In India, there are no comprehensive data on burned area, number of fires, and areas of regeneration for fear of accountability (for more information, refer to http://www.fire.uni-freiburg.de/iffn/country/in/in_5.htm). Two assessments made by the Indian authorities estimated forest loss at 1.45 million hectares and 3.73 million hectares, quite a difference. Furthermore, evidence from active fire maps, derived from the AHVRR instrument show significant fire activity that needs to be confirmed with evidence of burned areas (for more information, refer to http://www.gvm.jrc.it/tem/wfw/wfw.htm). In Brazil, it is important to see if the method described in this paper is able to detect the well-documented deforestation fires that are occurring in the south of the legal Amazon. The same is true in other tropical forests, such as central Africa and southeast Asia, where for the latter region it is important to be able to verify estimates derived from other sources (for more information, refer to http://www.fire.uni-freiburg.de/iffn/country/id/id_35.htm). Burning of agricultural land is often not presented in national statistics that mainly focus on forested areas and the financial impact of fires in forests. This data set indicates burning activity in all vegetated regions and therefore the opportunity to assess the amount of residue burning and land clearance burning activities is available to the scientific community. Countries where it is believed agricultural residue burning occurs in some significance include Russia, Kazakhstan, Argentina, United States of America, Italy, and India. Finally, it is important for this study to highlight any limitations in the science of detecting the signal from the burned area and how this can be improved in the future. Therefore the data set described in this paper, while not perfect, is nonetheless timely and worthwhile.

2. Satellite Image Data Set

[8] Burned area mapping at a regional scale has been performed over different ecosystems using SPOT VGT imagery [*Eastwood et al.*, 1998; *Fraser and Li*, 2002]. At the global scale the ERS Along-Track Scanning Radiometer 2 (ATSR-2) has been used with some success to map burned areas for the year 2000 [*Kempeneers et al.*, 2002] through a project called GLOBSCAR initiated by the European Space Agency (ESA). In this project, two algorithms were applied globally to derive burned area products with the same resolution as the GBA-2000 products. These results make a valuable data set for comparison, and values are reported in this paper where this is possible (information on GLOBSCAR products can be found at http://www.geosuccess.net). The GLOBSCAR values reported for vegetation classes are related to the International Geosphere-Biosphere Program (IGBP) product [*Loveland et al.*, 2000]. In addition, reference is made to detections made by the nighttime overpass of the ATSR-2 satellite and reported in the ATSR-2 World Fire Atlas (information can be found at http://odisseo.esrin.esa.it/ionia/FIRE/AF/ATSR/). A more detailed comparison study between these products is presented in the paper by *Simon et al.* [2004].

[9] The VGT sensor was launched on board the European SPOT-4 platform in March 1998 (information on this satellite and sensor can be found at http://www.spot-vegetation.com). The multispectral registration is reported to be better than 0.2 km, the multitemporal registration better than 0.5 km, and the absolute geolocation better than 0.8 km. The across-track resolution is approximately 1.1 km at nadir. The data are projected and interpolated to a constant pixel resolution of approximately 1 km^2. The sensor acquires data in four spectral bands covering visible (0.43–0.47 μm corresponding to blue wavelengths; 0.61–0.68 μm corresponding to red wavelengths) and infrared (0.78–0.89 μm corresponding to near infrared; 1.58–1.75 μm corresponding to short-wave infrared) wavelengths. The 2200 km swath width allows imaging over large areas and a return frequency yielding global, daily coverage, apart from within the tropics where, owing to the satellite orbit characteristics and Earth's curvature, images of the same area are taken every 4 out of 5 days. The acquisition time is 10:30 AM local solar time in the descending mode. The spectral band in the visible blue region provides information on the state of the atmosphere (aerosol density) and is used to make atmospheric corrections to the data. The short-wave infrared band centered at 1.65 μm was found to be useful for burned area mapping [*Eastwood et al.*, 1998; *Eva and Lambin*, 1998]. *Trigg and Flasse* [2000, 2001] showed among others the relevance of VGT spectral bands to detect burned areas. The VGT time series used in this work was the daily surface reflectance (S1) product starting from 1 December 1999 to 31 December 2000. Atmospheric corrections are performed by the Centre National d'Études Spatiales (CNES) using the Simplified Method for Atmospheric Corrections (SMAC) described in the work of *Rahman and Dedieu* [1994]. The expected improvement of the GBA-2000 product is that a number of

ecosystem specific regional algorithms have been developed by a network of partners and applied at the global scale at a resolution of 1 km and presented in a format easily utilized by a number of scientific communities.

3. Algorithms and Methodology

[10] The approach taken utilized a network of partners for the development and testing of a series of regional algorithms for processing the daily VGT-S1 imagery into burned area maps. This approach was adopted because the methods required to detect a burned area differ from one ecosystem or climatic zone to another (e.g., boreal forest, tropical forest, grasslands). The approach taken brought together different research groups with regional expertise to produce a global product. Furthermore, we wanted to avoid the use of a single or double algorithm for mapping the global product, as this work was being undertaken elsewhere by the European Space Agency (GLOBSCAR). Eleven regional algorithms in total were developed from temporal and spatial subsets of VGT S1 data. The main specifications of the algorithms, including the geographical regions used to develop the algorithms, are presented in Table 1. The naming convention of the algorithms was such that the institute, and in some cases also the developer, was associated with the algorithm was used. Table 1 provides reference information for each algorithm developed under the GBA-2000 initiative. Following a series of tests comprising intercomparisons of products derived from different algorithms over the same area, implementation of algorithms outside their region of development, and the ability of the algorithms to detect burned areas in different vegetation types, nine algorithms were selected for processing the entire year 2000 data set and integrated into a global processing chain [*Tansey*, 2002]. Two algorithms were not selected because a single algorithm adequately mapped burned areas in both northern and southern Africa, and a decision was made to use only one algorithm to map the African continent. It is shown that a number of the algorithms used daily VGT data to yield daily burned area products, e.g., IFI and GVM (Boschetti), while others used image compositing techniques to reduce levels of signal noise observed in the daily data, e.g., GVM (Stroppiana), UOE/UTL, and CCRS. The compositing methods are fully described by *Tansey* [2002], *Stroppiana et al.* [2002], and *Cabral et al.* [2003].

[11] The removal of contaminated pixels prior to applying the algorithms was an important stage in the image processing. A complete overview of the preprocessing steps, summarized in this paragraph, is given in the work of *Tansey* [2002]. Contaminated pixels having values characteristic of clouds, cloud shadow (that have similar spectral characteristics to burned areas), and fire smoke are removed. Those pixels located at the very edge of the image swath are removed because often they have erroneous values caused by the resampling method and also those that appear to be saturated (or have very high values of reflectance) in the short-wave infrared band caused by problems with the sensor. In addition, those pixels located in regions of pronounced topographical variation at the scale of 1 km, such as the Himalayas and the Andes, were removed because they were indicated as being burned when in fact they were areas of terrain shadow. A digital elevation model (DEM) called the Global Land One-km Base Elevation (GLOBE) was used to determine those pixels, using a method outlined by *Colby* [1991], whose spectral characteristics may have been contaminated with terrain shadow [*Hastings and Dunbar*, 1998].

[12] A global land cover product was used, first as a mask to remove nonvegetated surfaces (water, urban areas, deserts, and ice masses) and second to derive the estimates of burned area according to vegetation type presented in this paper. A vegetation mask was used because there were uncertainties concerning the performance of the algorithms in nonvegetated regions. These uncertainties were related to observations of dark rocks (particularly in eastern Africa), flooded salt pans, and melting snow and ice. The following regions were excluded from the analysis: extensive regions of the Sahara Desert and central Saudi Arabia, the Atacama Desert in South America, regions of Iran and southern Pakistan, the Tibetan Plateau and small regions of central Australia and western United States. A number of global land cover products are available to the scientific community, although unfortunately, each product has a different number of classes, having been derived using different methods and having been developed with different user applications in mind. The critical point to stress here is not directly the choice of land cover product, but to understand the reasons for choosing the product and to state any modifications that have been made to the land cover product. The global land cover product selected for this study was the University of Maryland (UMD) global land cover product [*DeFries et al.*, 1998; *Hansen et al.*, 2000]. The nonvegetation mask was applied to all regions of the globe in a consistent manner.

[13] The global data set was distributed into sections depending on large-scale vegetation features, seasonal burning activity, or to ensure problem-free computational processing. The selection of a suitable algorithm for operational implementation outside regions of algorithm calibration described in Table 1 was made after looking at three criteria. The first criterion was to look at the main types, distribution, and patterns of vegetation in the region using a global land cover map and to select an algorithm or number of algorithms that had been developed and successfully applied over a region with similar characteristics. The second criterion was then to apply these algorithms to the area under consideration and to see how they compared between themselves and also compared to other sources of burned area or active fire information. The third criterion depended on certain characteristics of the region of interest such as topography, presence of agricultural areas, areas tending to flood, and urban areas that can all have an influence on the algorithm's results. All of the criteria above were considered when finding a suitable algorithm for the detection of burned areas outside regions of development. In some regions a single algorithm was assumed to adequately detect burned areas, mainly owing to the region having similar characteristics to the region of algorithm development. In other regions it was necessary to use two algorithms to fully capture all of the burning activity for a number of reasons. These include circumstances where burning activities occur in two or more distinct vegetation types, such as in northern North America, where one algorithm is used to detect scars

Table 1. Main Characteristics of the GBA-2000 Burned Area Algorithms

Algorithm	Overview of Main Characteristics	Region of Development	Reference
CCRS Canada Centre for Remote Sensing, Canada	Ten-day composites are derived with a max. NDVI[a] criteria. A multiple logistic regression model based on ten-day changes, an ecosystem mask and monthly satellite-derived metrics is used. The products are filtered and region grown.	one region of Canada: 62.5°–57°N; 112°–104.5°W (SPOT VGT S10[b] data from the year 1998 were also used)	*Fraser et al.* [2003]
CNR Institute for Electromagnetic Sensing of the Environment, Italy (not used[g])	Contextual supervised classification methodology based on hierarchical use of the MultiLayer Perceptron (MLP) neural network which use the spatial and temporal information of daily images to produce daily maps of burned areas.	one region of Africa: Africa: 18°N–0°S; 20°W–55°E	*Brivio et al.* [2002]
GVM (Boschetti) Global Vegetation Monitoring Unit, JRC, Italy	Removal of contaminated[c] pixels and a BRDF[d] model is inverted to yield reflectance. A change detection method[d] is used to compare values predicted from the model and observed in the NIR[a] and SWIR[a] bands.	two regions of Central America: 22°–7°N; 93°–77°W 33°–15°N; 117°–93°W	*Tansey* [2002] *Boschetti* [2003]
GVM (Stroppiana) Global Vegetation Monitoring Unit, JRC, Italy	Removal of contaminated[c] pixels and composited over a ten-day time period using the minimum NIR[a] value. The algorithm uses CART[e] theory to derive decision rules from training sets. The resulting products are filtered and summed to create monthly products.	one region of Australia: 11°–21°S; 125°–135°E	*Stroppiana and Grégoire* [2002] *Stroppiana et al.* [2002, 2003]
IFI International Forest Institute, Russia	Removal of contaminated[c] pixels, daily values of the NIR[a] band are observed for abrupt changes when compared with an intermediate product and other tests are satisfied.	two regions of Russia: 68°–60°N; 45°–60°E 60°–48°N; 118°–140°E	*Ershov and Novik* [2001]
NRI Natural Resources Institute, UK (not used[g])	A change detection algorithm using preburn and postburn data in the NIR[a] and SWIR[a] bands. The preburn image is updated daily with noncontaminated pixels. To reduce the variation of the spectral signal caused by viewing geometry the algorithm utilizes daily data in five-day cycles.	one region of southeastern Africa: 17°–29°S; 11°–30°E	*Boschetti et al.* [2002]
UOE/UTL University of Evora, Portugal; Technical University of Lisbon, Portugal	Removal of contaminated[c] pixels and composited over a month using the 3rd min. NIR[a] value. The algorithm uses CART[e] theory to derive decision rules from training sets.	one region of Brazil: 5°N–20°S; 75°–45°W	*Silva et al.* [2002]
UTL – Africa 1 UTL – Africa 2 UTL – Europe UTL – Asia Technical University of Lisbon, Portugal	Removal of contaminated[c] pixels and composited over a monthly time period using the minimum NIR[a] value. Africa 2 uses CART[e] theory to derive decision rules. The other algorithms use Fisher's linear discriminant analysis[f] approaches but use different thresholds.	four regions were provided: Africa A: 10°–28°S; 22°–42°E Africa B: 18°N–35°S; 20°W–55°E Europe: 44°–35.5°N; 10°W–0° Asia: 55°–40°N; 115°–135°E	*Silva et al.* [2002, 2003]

[a]NIR refers to the near infrared band, SWIR refers to the short-wave infrared band. NDVI refers to the normalized difference vegetation index.
[b]SPOT VGT S10 data refers to products that have been composited over a ten-day period following a maximum NDVI criteria.
[c]Contaminated pixels are those of cloud or smoke, cloud shadow, acquired at extreme angles, sensor saturation in the SWIR band, nonvegetated or in topographic shadow.
[d]BRDF refers to the bidirectional reflectance distribution function. The BRDF model is described by *Roujean et al.* [1992]. The method is adapted from *Roy et al.* [2002].
[e]CART is an acronym for Classification Trees and Regression Trees, described by *Breiman et al.* [1984].
[f]Fisher's Linear Discriminant Analysis method is described in the work of *Johnson and Wichern* [1988].
[g]Not used indicates that this algorithm was used to create the final GBA-2000 product.

in boreal forests and another is used to detect scars in shrublands and evidence of burning activity in daily images (smoke or active fires observed) or through using higher-resolution images such as from Landsat Thematic Mapper (TM) (available from http://Glovis.usgs.gov/BrowseBrowser.shtml) to determine that burned areas are not adequately detected by one algorithm but by combining the detections from two algorithms. Specific improvements are made by using two algorithms to improve the detections made in the USA and Central America, central and eastern Asia, southern Europe, and northern Africa.

[14] After the tests described above had been carried out, the global data set was processed using the following method. Please refer to Table 1 for a description of the acronyms used in this paragraph. Australia was processed with an algorithm developed by GVM (Stroppiana). The IFI algorithm was used solely to process the southern half of South America (including Argentina and Chile), northern Europe, the majority of northern Asia (including most of Russia), the Indian subcontinent, and continental and insular southeast Asia. The IFI algorithm was used together with the GVM (Boschetti) algorithm (i.e., both products were

merged) for regions of the United States (US), south of 30°N, and Central America, the UTL Europe algorithm in southern Europe and northern Africa, the UTL Africa 2 algorithm in Turkey, Iraq, and regions surrounding the Black and Caspian Seas, and the UTL Asia algorithm (a derivative of UTL Africa 1) for a region from the Tibetan Plateau, through Mongolia, and northern China to Japan. The CCRS algorithm was used to derive burned area products for forested regions of Canada and the US, north of 30°N (according to a forest cover map provided by CCRS). The nonforested regions of the US, north of 30°N, were processed using the first algorithm developed by the UTL group (UTL Africa 1). The UOE/UTL algorithm was used to process a window covering the northern half of the South American continent (including the Amazon Forest). The UTL Africa 2 algorithm was used to derive the burned area products for sub-Saharan Africa. In certain regions, such as New Zealand, some Pacific Islands, northern England, Scotland, Eire, Northern Ireland, Hawaii, Iceland, and Greenland, the algorithms were not applied. This was due either to their isolated location or their insignificant contribution to global burning activity.

[15] In certain locations, algorithms were not applied to the VGT data set for the whole of the year 2000. This depended on whether there was a distinct fire season, caused mainly by climatic variations (snow cover, heavy rainfall, etc.), or significant commission of burned areas outside the main periods of fire activity such as that caused by flooding. To determine the main periods of burning activity, information was used from published literature such as *Dwyer et al.* [1999], *Cahoon et al.* [1992], *Dwyer et al.* [1998], *Moreno-Ruiz et al.* [1999], and that available through the International Forest Fire News: Country Notes Web site at http://www.fire.uni-freiburg.de/iffn/country/country.htm. The data processing started at least 1 month before the indicated start of the fire season and one month after the end of the fire season. To summarize, data were processed between April and October 2000 for regions lying north of 30°N, January to May 2000, and September to December 2000 between 30°N and 8°N in Central America, 30°N and 10°N in Africa, and 30°N and 6°N in India and southeast Asia and from April to December 2000 in southern Africa, between approximately 10°S and the Cape of Good Hope in South Africa. The complete year 2000 data set was processed for all other regions including South America south of 10°N, equatorial Africa between 10°N and 10°S, and insular southeast Asia and Australia south of 6°N.

[16] It is generally assumed that a vegetated area is burned only once during a fire season. However, over the observation period of this study, it was possible that the same vegetated area burns twice. This can occur in regions between 0° and 30°N in all continents. For example, a vegetated area was burned toward the end of the 1999–2000 dry season and was detected in January 2000, and after the wet season the vegetation was burned again earlier in the 2000–2001 dry season and was detected in December 2000. In the data set presented, the year 2000 synthesis product provides an estimate of the area burned during the year 2000. However, for this particular product, a value is associated to each pixel indicating if it has been detected as burnt or not burnt, and not if the pixel has been detected as being burnt twice. For those regions described previously in this section, the actual annual burned area is calculated by summing the monthly estimates. It is important for the user to be aware of this to ensure the correct data is used for their application.

[17] Throughout the implementation of the regional burned area algorithms, care was taken to ensure that no large errors of commission or omission were made. Confirmation of burning activity was made using quick-look Landsat TM imagery or evidence of burning activity in the VGT products such as smoke and fire fronts. In all but one case, there was no overlap area at the boundaries of the regionalized algorithms. In the single overlap region, located in northern Australia and southern Indonesia, correspondence between the two burned area maps, produced with the IFI and GVM (Stroppiana) algorithms, was good. No major errors were observed at the join between regions. Artificial edge effects, however, are observed in central southern Russia near to the Kazakhstan border, caused by the inherent properties of the IFI algorithm that uses data windows 200 × 200 km in size to generate statistics of burned areas. After an investigation, these errors were believed to be caused by contamination of the VGT S1 image data owing to thin smoke or during the raw data processing not masked out during the various data cleaning processes applied to the data. These errors are only observed in the region of southern Russia, and given that the IFI algorithm is used extensively elsewhere with no further occurrences reported, it was decided to accept these errors in the final product.

[18] The UMD land cover product was used to present the estimates of burned area according to vegetation type. At the time of the project's execution, it was considered to be the most current product that was freely available to the users, actively being used by many different research groups and not containing a large number of classes (the UMD product is available from http://glcf.umiacs.umd.edu/data). The UMD product has 14 classes, of which 11 indicate a vegetation cover. The vegetation classes represented are evergreen needleleaf, evergreen broadleaf, deciduous needleleaf, deciduous broadleaf and mixed forest, woodland, wooded grassland, closed shrubland, open shrubland, grassland, and cropland. However, to estimate the biomass burned and gas emissions from 11 classes of vegetation requires a considerable amount of information, such as biomass loading, burning efficiencies, and emission factors for each class. Therefore we grouped the 11 vegetation classes in the UMD product into four groups. We justified the grouping of the vegetation classes presented in this paper partly on the basis of evidence presented in the literature. Studies describing continental and global estimates of burned biomass and emissions report parameter values (e.g., burning efficiency, biomass loadings, emission factors, fuel moisture, fire intensity) that are averaged (or simplified) for the purposes of modeling studies using vegetation types such as wetlands, savanna, and boreal ecosystems in the work of *Cofer et al.* [1996], tropical forest, tropical savanna, temperate and boreal forest, fuelwood, and agricultural residues in the work of *Hao and Ward* [1993] and *Granier et al.* [2000] (with the replacement of tropical savanna with savanna) or savanna and grasslands, tropical forest, extratropical forest, biofuel burn-

ing, and agricultural residues as presented in the work of *Andreae and Merlet* [2001]. At this level of detail, *Granier et al.* [2000] used these classes to derive a 3-D chemical transport model to assess the significance of biomass burning on the ozone budget. Furthermore, the literature often reports burned biomass and gas emission values for vegetation types having regional naming conventions or those that are not easily translated at larger scales, such as Fynbos and infertile savanna given in the work of *Scholes et al.* [1996b]. The results presented in this paper are illustrative of the burning of broad vegetation classes at the global scale. For biomass burning and emission studies requiring a greater level of detail with regard to burning in specific vegetation types, the GBA-2000 product can be used with more precise land cover products, biomass, and emission parameters. An example of the use of the GBA-2000 product can be found in the paper by *Hoelzemann et al.* [2004]. As previously mentioned, the 11 UMD classes were assigned to one of four broad vegetation groups. Evergreen needleleaf, deciduous needleleaf, and mixed forests were grouped into a class called needleleaf and mixed forests (N&MF); evergreen broadleaf and deciduous broadleaf were grouped into a class called broadleaf forests (BF); woodland, wooded grassland, closed shrubland, and open shrubland were grouped into a class called woodlands and shrublands (W&S); and grasslands and croplands (G&C) were merged to form the fourth class. To enable the users to gain confidence in using the burned area estimates reported for each vegetation group, the variation of parameter values used to estimate burned biomass and emissions should be kept to a minimum. From a practical point of view, this variation is difficult to measure as there are potentially numerous sources of information to consider. Therefore only a brief overview is provided in this paper. For each of the four vegetation groups, values of emission factors, combustion efficiencies, and average biomass loadings have been taken from literature for land cover classes having similar labels and properties to the UMD classes. Maximum aboveground biomass loads (kg/m^2) range between 27.5 and 38.4 for N&MF, 22.0 and 27.5 for BF, 2.7 and 10 for W&S, and 1.6 and 3.8 for G&C taken from *Zheng et al.* [2003] and *Palacios et al.* [2002]. Estimates of combustion efficiency (used when calculating emissions using emission ratios) range between 0.87 and 0.88 for N&MF, 0.87 and 0.89 for BF, 0.92 and 0.97 for W&S, and 0.9 and 0.96 for G&C taken from *Hao and Ward* [1993], *Scholes et al.* [1996b], and *Kaufman et al.* [1992]. Estimates of emission factors (grams/kg biomass) for CO_2 range between 1569 and 1640 for N&MF, 1569 to 0.89 for BF, 1530 to 1613 for W&S, and 1515 to 1613 for G&C taken from *Andreae and Merlet* [2001] and *Ferek et al.* [1998]. To aid the interpretation of the burned area maps, the grouped vegetation cover product was overlain with a political boundary map.

4. Analysis and Discussion of Global Vegetation Burning

[19] Information on the spatial and temporal distribution of biomass burning is very much in demand by the climate and ecosystem modeling communities. Therefore the GBA-2000 product has been made available to users at no cost (available at http://www.gvm.jrc.it/fire/gba2000/index.htm). Maps of the GBA-2000 products can be viewed interactively through the United Nation Environment Programme (UNEP) Internet Map Server site (available at http://www.grid.unep.ch/activities/earlywarning/preview/ims/gba/). On the UNEP site the user can overlay land cover maps, political boundaries, and protected regions with the software tool provided. The data set described in this paper consists of annual burned area estimates for the four vegetation classes outlined in the previous section differentiated by political boundary. A description is given of the spatial and temporal distribution of burned areas for each of broad vegetation zone in the year 2000. An example of the use of the monthly burned area products is presented for the Central African Republic (CAR) and illustrates the usefulness of the data set for the monitoring of burning activity and assessing the impact of burning on the vegetation. The burned area estimates presented in this paper were derived using a dedicated software tool, developed by the European Commission Joint Research Centre (JRC) and the University of Alcala, Spain, and called the Global Fire Analysis GIS Module. The module, run using ESRI's ArcView software, computes and tabulates burned area statistics for any region of interest or corresponding ancillary map (such as land cover and political boundary). Estimates of burned area are given in square kilometers (km^2). In the following paragraphs the use of the phrase "burning activity" refers to the detection of burn scars and not the detection of active fires or fire activity.

4.1. Spatial and Temporal Distribution of Vegetation Burning

[20] Estimates of burned area (in square kilometers) are given in Table 2 by grouped vegetation type and political boundary. In addition to the burned area values, figures are presented on the number of burned scars (either single pixel or cluster of pixels) and the percentage of the total area of that vegetation type burned within the specified country. The values given in Table 2 are comma delimited and are presented for the year 2000 product only. A zero (0) in the table indicates that no burned areas were detected in that particular vegetation type, a dash indicates that the vegetation group is not represented in that particular country. Monthly data are available for each country, but because of the magnitude of this data set, only the annual synthesis is shown. Only those countries with burned areas greater than 60 km^2 in the year 2000 are presented; those countries with total burned areas less than 60 km^2 contributed a very small percentage of the global burned area ($\approx$0.02%). Before a detailed interpretation of the distribution of burned areas is given, it is worth extracting the main themes from Table 2.

[21] The estimated global burned area for the year 2000 is just over 3.5 million km^2, and nearly 600,000 separate burn scars were detected. Of the total area burned, 1.5% is classified as N&MF, 1.2% as BF, and 16.6% as G&C. The most common type of vegetation burned is W&S at 80.7%. However, this class only represents 61% of the total number of burn scars. The percentage of the total number of burn scars are 2.5% for N&MF, 2.9% for BF (a total of approximately 100,000 km^2 for forests), and 33.9% for G&C. The GLOBSCAR product reported a global total of approximately 2 million km^2, of which 307,000 km^2 were

Table 2. Burned Area Estimates (km^2) Reported for Country and Vegetation Type for the Year 2000[a]

Country	Needleleaf/Mixed Forest	Broadleaf Forest	Woodlands/Shrublands	Grasslands/Croplands
Afghanistan	6,6,1.5	0	336,193,0.1	344,207,0.3
Albania	49,26,4.2	2,1,1.6	50,44,0.5	24,21,0.1
Algeria	126,43,9.0	2,2,1.8	1264,237,0.7	128,91,0.3
Angola	-	2706,1290,6.2	271789,21077,25.5	22006,8459,20.6
Argentina	164,167,0.5	1063,615,1.4	47113,13931,2.3	7146,4875,1.4
Armenia	11,6,1.3	4,3,1.5	56,33,0.8	30,23,0.2
Australia	345,249,1.7	4101,1219,1.7	525357,20303,8.3	28982,9083,3.3
Austria	59,41,0.2	0	21,25,0.1	17,15,0.1
Azerbaijan	44,24,1.4	45,26,1.9	109,85,0.4	337,124,0.6
Bangladesh	-	0	12,9,0.0	265,54,0.3
Belarus	4,7,0.0	0	151,163,0.2	306,286,0.2
Benin	-	2,1,18.1	10614,1194,14.4	2400,689,5.8
Bhutan	48,31,0.3	8,8,0.1	82,36,0.9	16,10,1.0
Bolivia	37,34,0.6	2462,876,0.5	4616,1797,1.1	3005,759,3.6
Bosnia and Herzegovina	60,37,0.5	1,2,0.0	134,50,0.7	171,45,1.0
Botswana	-	0	31156,6607,6.3	2400,1144,3.6
Brazil	17,17,0.0	829,361,0.0	12125,3638,0.3	5258,1575,0.8
Bulgaria	69,38,0.7	21,15,0.7	228,184,0.9	1811,634,2.6
Burkina Faso	-	2,1,66.5	15136,2522,5.9	603,395,4.5
Burundi	-	24,15,3.5	492,174,2.9	193,86,2.7
Cambodia	-	60,33,0.3	3080,348,2.8	710,196,1.7
Cameroon	-	499,284,0.3	45291,3771,18.1	4344,1670,9.4
Canada	1555,300,0.1	48,8,0.1	3773,542,0.1	183,103,0.0
Central African Republic	-	569,349,1.6	183153,7804,31.7	1803,1024,33.0
Chad	-	2,2,16.7	77725,10272,14.2	2499,1479,10.8
Chile	56,56,0.1	9,9,0.0	2103,1105,0.7	372,336,0.5
China	8801,2941,1.5	1669,904,1.4	28809,11238,0.7	23543,8427,0.7
Colombia	6,5,0.1	42,31,0.0	1629,614,0.4	8015,735,4.6
Congo	-	571,191,0.3	2669,685,2.6	2545,702,4.3
Cote D'Ivoire	-	7,5,0.1	17197,1499,8.1	3628,1381,3.8
Croatia	7,9,0.1	22,10,0.4	18,17,0.1	114,60,0.5
Cuba	0	9,8,0.1	277,120,0.4	225,93,0.8
Democratic Republic of the Congo	-	12786,4861,1.1	221229,18269,22.3	26259,8550,22.2
Djibouti	-	-	290,51,11.2	131,44,13.2
Ecuador	0	1,1,0.0	98,73,0.1	69,53,0.1
Egypt	-	-	206,110,0.9	706,143,2.5
Eritrea	-	-	2256,1141,4.6	1407,649,9.6
Ethiopia	-	1033,427,3.4	100040,15242,14.6	34811,9773,12.0
Finland	15,11,0.0	0	81,142,0.0	2,3,0.0
France	175,92,0.3	17,17,0.1	228,155,0.1	129,88,0.0
Gabon	-	19,10,0.0	222,111,0.4	589,208,1.5
Gambia	-	-	680,148,8.5	160,76,8.5
Georgia	42,27,0.5	1,2,0.0	56,44,0.2	66,35,0.2
Germany	12,4,0.0	0	23,20,0.0	32,26,0.0
Ghana	-	11,7,0.1	43000,2824,27.6	10979,2658,17.7
Greece	47,31,0.6	0	595,119,1.1	527,197,0.9
Guatemala	10,9,0.2	36,18,0.1	81,54,0.2	22,21,0.3
Guinea	-	33,11,0.8	6597,1863,3.5	1365,519,2.7
Guinea-Bissau	-	0	308,109,1.3	94,65,1.4
Hungary	1,1,0.2	0	82,78,0.7	1297,545,1.7
India	264,127,0.5	162,95,0.2	43286,3446,2.1	3330,1577,0.5
Indonesia	-	148,50,0.0	1199,223,0.2	533,156,0.2
Iran	211,108,2.3	74,47,2.4	320,190,0.1	395,232,0.2
Italy	84,54,0.2	48,21,0.4	421,318,0.4	1968,707,1.4
Japan	542,239,0.4	57,45,0.3	454,221,0.3	124,85,0.2
Kazakhstan	89,50,1.0	8,10,1.0	6835,3980,0.8	74098,17378,4.6
Kenya	-	563,187,3.9	33043,7804,12.5	24191,7225,10.3
South Korea	1149,349,2.7	927,216,4.1	434,265,1.2	133,80,0.8
Kyrgyzstan	25,15,1.7	4,5,2.1	334,262,0.5	695,363,0.7
Laos	51,28,0.9	287,107,0.2	632,200,0.7	501,95,3.0
Lesotho	-	4,4,5.8	1316,585,6.0	464,282,5.4
Macedonia	25,14,1.3	1,1,0.2	66,48,0.7	72,57,0.6
Madagascar	-	179,100,0.2	5272,2610,1.8	5885,2544,2.7
Malawi	-	287,77,6.1	4564,1335,5.7	468,225,5.1
Mali	-	-	20678,5660,4.8	1082,674,5.8
Mauritania	-	-	16844,1710,20.9	18,8,10.8
Mexico	475,348,1.5	583,393,0.3	16911,6070,1.2	3247,1827,1.1
Moldova	0	0	67,74,3.3	1009,532,3.3
Mongolia	1217,375,3.5	3,5,1.2	8108,2490,1.0	16618,1647,2.9
Morocco	0	0	1534,522,0.7	713,316,1.3
Mozambique	-	1106,541,7.2	97843,11393,13.7	3904,2122,11.4
Myanmar	92,34,0.4	600,234,0.3	8688,945,2.4	1679,522,2.0
Namibia	-	1,1,100.0	33720,9143,5.8	1370,989,4.2

Table 2. (continued)

Country	Needleleaf/Mixed Forest	Broadleaf Forest	Woodlands/Shrublands	Grasslands/Croplands
Nepal	453,264,4.1	50,37,3.2	1682,600,2.2	796,431,1.7
Niger	-	-	3201,990,1.1	214,143,12.0
Nigeria	-	21,17,0.2	26776,7152,4.2	5101,2548,2.1
Norway	27,22,0.1	0	127,133,0.1	6,11,0.0
Pakistan	50,36,1.3	6,3,3.6	241,168,0.1	110,72,0.1
Papua New Guinea	-	34,13,0.0	74,27,0.1	24,8,0.1
Paraguay	0	248,102,0.3	1018,266,0.3	50,27,0.4
Peru	38,36,0.3	78,64,0.0	3133,1943,1.2	3127,1435,1.5
Poland	29,25,0.1	39,13,3.4	67,68,0.1	28,31,0.0
Portugal	20,16,0.7	0	656,250,1.1	205,132,0.7
Republic of Korea	288,42,1.4	125,25,0.8	60,40,0.2	38,25,0.2
Romania	806,199,3.1	132,78,2.2	476,348,1.2	2192,887,1.4
Russia	29846,6874,0.8	1162,618,1.0	90237,50348,0.9	101118,39687,4.0
Rwanda	-	51,31,2.4	276,88,1.7	208,81,3.7
Senegal	-	-	10440,2130,6.5	886,489,6.3
Serbia and Montenegro	86,46,1.2	23,14,0.5	80,61,0.3	439,202,0.8
Slovakia	70,34,0.9	51,22,1.0	31,29,0.2	17,14,0.1
Somalia	-	0	13498,3758,5.8	4768,2086,3.4
South Africa	-	268,186,2.8	50514,18981,5.8	22669,9951,8.5
Spain	113,44,0.4	4,4,0.1	1031,501,0.4	535,353,0.3
Sudan	-	1031,396,22.0	379901,19260,29.0	23414,8563,35.3
Swaziland	-	15,8,2.3	391,121,2.9	69,55,2.3
Sweden	19,20,0.0	0	81,108,0.0	3,6,0.0
Tajikistan	0	0	110,75,0.2	337,173,0.7
Tanzania	-	4378,1536,7.0	103679,14373,14.8	14115,6135,12.0
Thailand	-	0	929,253,0.4	1043,328,0.4
Togo	-	10,6,18.9	4517,888,14.6	1866,481,7.2
Tunisia	6,5,2.7	0	44,13,0.1	24,16,0.1
Turkey	22,23,0.2	7,5,0.1	819,492,0.3	1922,596,0.4
Turkmenistan	0	-	63,30,0.0	178,32,0.4
Uganda	-	893,320,4.0	26096,2258,,17.5	4459,1660,13.8
Ukraine	102,48,0.9	59,39,2.6	2940,2056,3.2	18809,6579,4.1
United States of America	5867,1344,0.5	146,115,0.0	17302,6739,0.4	11648,5496,0.4
Uruguay	-	0	46,33,0.1	38,34,0.0
Uzbekistan	0	-	157,123,0.1	361,204,0.3
Venezuela	5,3,0.5	115,68,0.0	2791,841,0.9	3563,673,2.4
Vietnam	13,8,0.1	12,11,0.0	266,72,0.2	92,46,0.1
Zambia	-	1,1,1.7	101967,13654,14.9	8385,3971,15.3
Zimbabwe	-	-	15552,2936,5.0	2041,968,2.7

[a]Burned area (km^2), number of scars and % of each vegetation type per country burned (comma delimited). A dash (-) indicates that the vegetation is not present in the country, a zero (0) indicates no burned area was detected in that vegetation.

classified as forest (forest area derived from IGBP). Estimates given by *Levine et al.* [1999] are between 5–5.6 million km^2 globally, 300,000–550,000 km^2 in forests, and 5 million km^2 in woodlands and savannas.

[22] The country and vegetation class making the largest contribution to the global burned areas is Australian W&S, with approximately 525,000 km^2 that accounts for 8.3% of this class. This country and vegetation class alone accounts for 15% of the global annual burned area. In N&MF, burning in Russia (≈30,000 km^2) makes up 55% of the total area burned in this grouped class. Canada contributes 3% of the total burned area in this class. In BF, burning in DR Congo (≈13,000 km^2) contributes 30% of the total burned area in this class. Rather surprisingly, Brazil contributes only 2% to the total burned area in the BF class. Reasons for the apparent low values estimated in Brazil and also Canada are discussed later in this paper. In the G&C class, burning in Russia (≈101,000 km^2) contributes 17% of the total burned area in this class, Kazakhstan (13%) and Ethiopia (6%) follow behind.

[23] The country and vegetation class in which burning has the greatest influence can be assessed in terms of the percentage of the total area of the vegetation within the country that has been burned. After excluding those classes without adequate representation of vegetated pixels indicated as being burned (those less than 30 pixels in this analysis), the table is dominated by the African nations. At the top is Sudan with burning activity affecting 22% of the BF area, 29% of the W&S, and 35% of the G&C areas. Other countries where burning activity occurs widely in vegetation classes W&S and G&C are Angola, the Central African Republic, Ghana, and the DR Congo. According to the statistics of BF, 19% has burned in Togo, 22% in Sudan, and 7% in Togo. The percentage of BF affected by fire in Brazil is rounded to one significant figure to 0.0%. In N&MF, 9% is affected in Algeria. The percentage of forest affected in Canada and Russia are estimated to be 0.1 and 0.8%, respectively.

[24] At the continental scale, in terms of area, Africa contributes 64% of the global total, compared to 59% reported by the GLOBSCAR product. The GLOBSCAR product estimates the total burned area to be a factor of two lower than that reported by the GBA-2000 product. Australasia (Australia and Papua New Guinea) contributes 16%, Asia (including Russia) 14%, South America 3%, North America 2%, and Europe 1%. In terms of the number of burn scars detected, Africa contributes 54%, Asia 27%, South America 6%, Australasia 5%, North America 4%, and

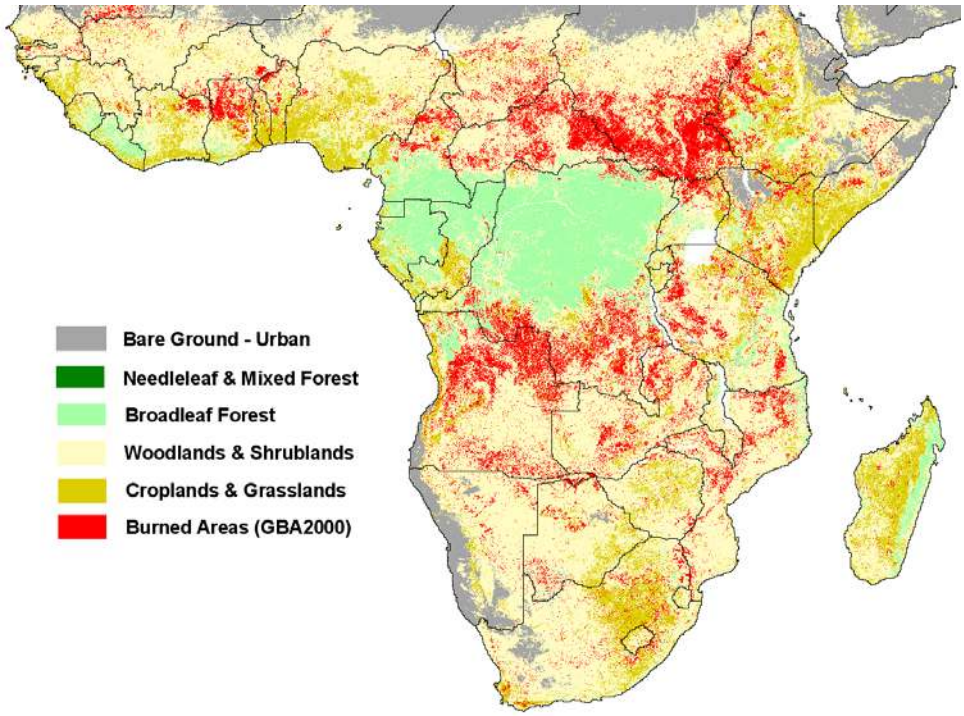

Figure 1. Burned area and grouped UMD vegetation map for sub-Saharan Africa in the year 2000 (scale 1:20,000,000).

Europe 3%. After examining more closely the burning of vegetation in Africa (a total of 2.3 million km^2), we see that 88% (≈1.98 million km^2) of the burned areas in Africa are classed as W&S, 11% are G&C (≈246,000 km^2), and only 1% are classed as BF (≈27,000 km^2). In fact, the burning of W&S in Africa makes up over half of the global burned areas in the year 2000 and nearly 40% of the total number of individual burn scars detected. Estimates reported from the GLOBSCAR product are 1.2 million km^2 for continental Africa, 200,000 km^2 for African forests, approximately 1.7 million km^2 from *Scholes et al.* [1996a], and approximately 1.54 million km^2 from *Barbosa et al.* [1999]. In Europe, three-quarters of the burned area are classed as G&C (≈30,000 km^2), 18% as W&S (7655 km^2), and 6% as both forests classes (2302 km^2), compared to the GLOBSCAR product that estimates a total burned area of 57,500 km^2, of which 21,000 km^2 was estimated to be burning in forested regions. In Asia, burning of N&MF contributes 9% of the total area (≈43,000 km^2), W&S 42% (≈197,000 km^2), and G&C 48% (≈229,000 km^2); the remaining 1% is BF. The total amount burned is estimated at approximately 0.5 million km^2 compared with 0.2 million km^2 by the GLOBSCAR product. In South America, 4% of the total burned area is classed as BF (4847 km^2), 68% is classed as W&S (≈75,000 km^2), and 28% as G&C (≈31,000 km^2). In North America including Central America, 13% of the total area burned was classed as N&MF (7907 km^2), 62% as W&S (≈38,000 km^2), and 25% G&C (≈15,000 km^2). The total estimated burned area was approximately 62,000 km^2 compared to 111,000 km^2 from the GLOBSCAR product. In Australasia the burning activity is dominated by Australia with only a very small amount detected on Papua New Guinea. The Australia statistics can be approximated to the continental scale, presented in a section later in this paper. A number of maps are presented that show the spatial distribution of burn scar detection in the year 2000. In all of the figures presented, the grouped vegetation classes are shown as well as bare surfaces. The burned areas are shown in red. Figure 1 shows sub-Saharan Africa at a scale of 1:20,000,000. Figure 2 shows Europe and northern Africa at a scale of 1: 15,000,000. Figure 3 shows Asia at a scale of 1:27,000,000. Figure 4 shows insular southeast Asia and Australasia at a scale of 1:20,000,000. Figure 5 shows North America at a scale of 1:26,000,000. Figure 6 shows a section of South America at a scale of 1:23,000,000. Reference is made to these maps in the following sections.

4.2. A Regional Overview of Burning Activity in the Year 2000

[25] In this section, regional patterns of burning activity are described with reference to the vegetation classes presented in the previous section. Information on possible errors in the burned area maps is also presented. Most of this information is purely qualitative and has been derived by comparing visually burned area maps with quick-look Landsat TM products or looking for evidence of burning activity in the VGT product.

4.2.1. Southern Africa

[26] In southern Africa (see Figure 1), fire incidence is higher at the lower latitudes, especially in Angola and DR Congo. Fire incidence is lower in the southeast and very low in the semidesert and desert areas of the southwest. In the northwest, most burning took place during June through August, while in the east burning was concentrated in July through September. July was the peak month of the year 2000 fire season. The burned area map, shown in Figure 1, displays clear variations in the spatial pattern of burning. In

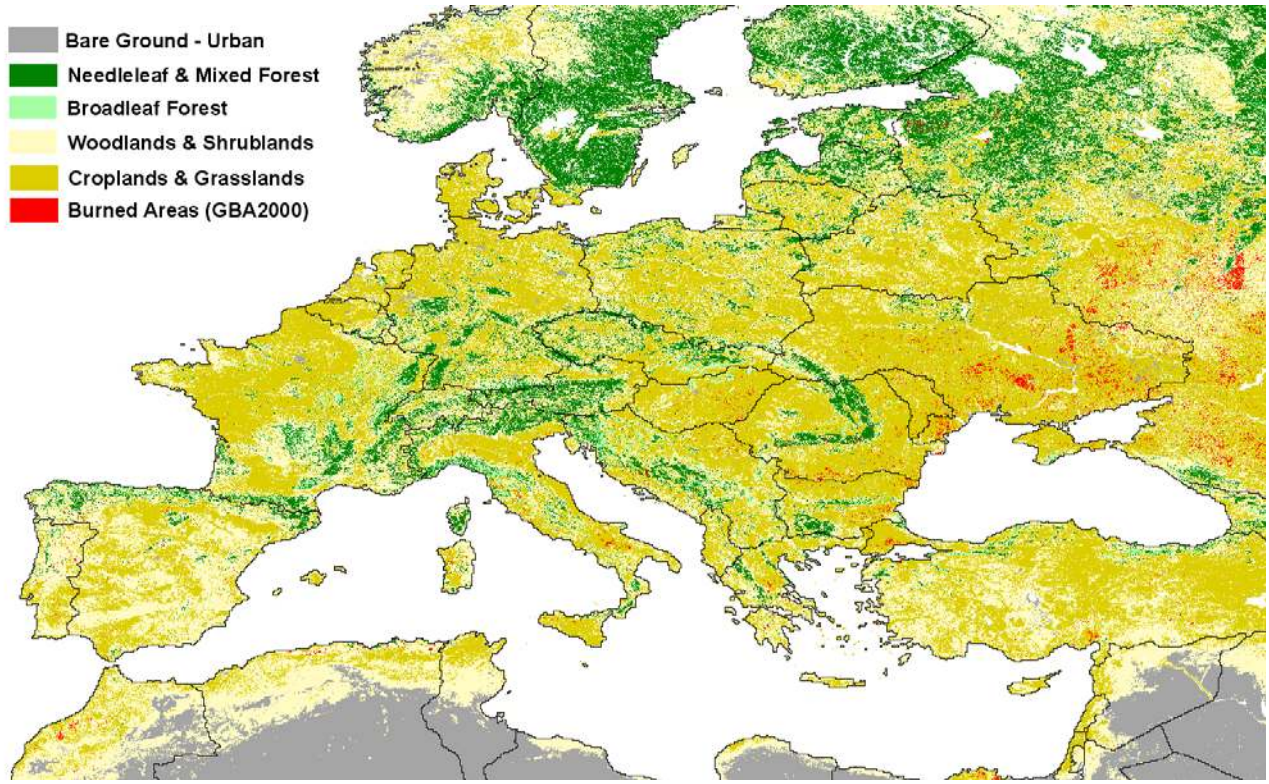

Figure 2. Burned area and grouped UMD vegetation map for Europe and northern Africa in the year 2000 (scale 1:15,000,000).

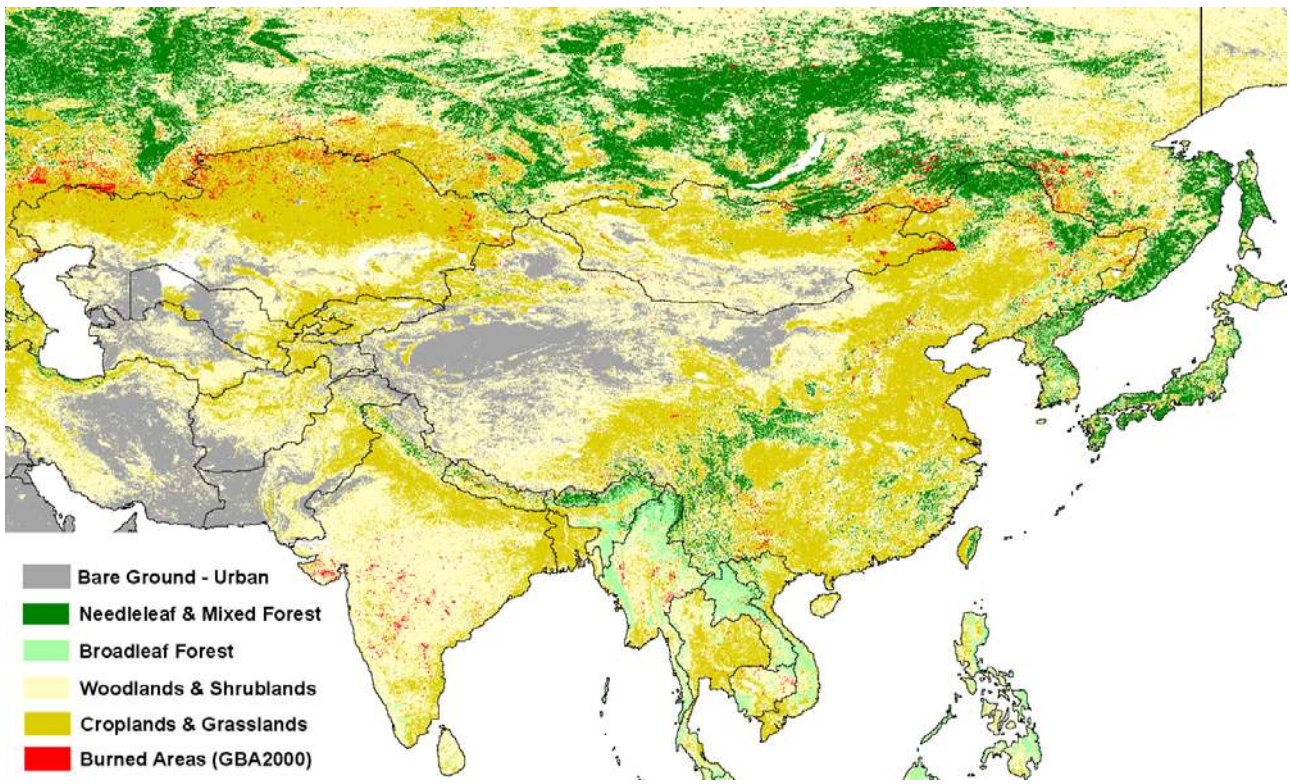

Figure 3. Burned area and grouped UMD vegetation map for Asia in the year 2000 (scale 1:27,000,000).

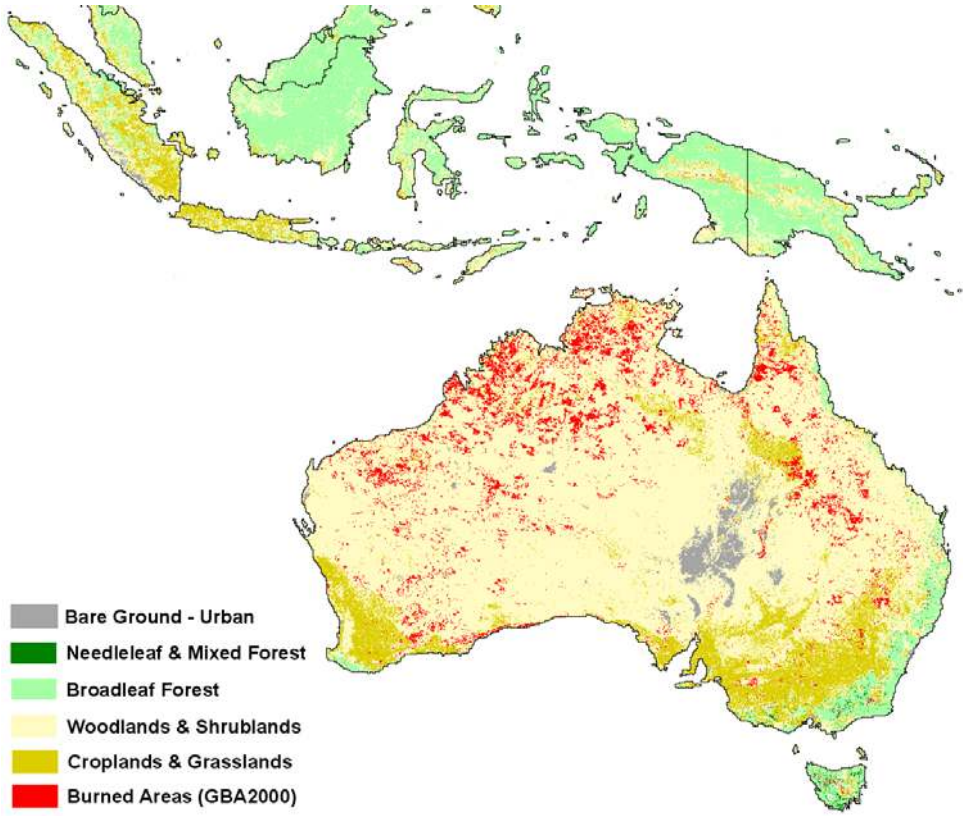

Figure 4. Burned area and grouped UMD vegetation map for insular southeast Asia and Australasia in the year 2000 (scale 1:20,000,000).

the northern part of the region, especially in northeastern Angola and southern DR Congo, by the end of the fire season, vast areas are continuously burned as a result of the coalescence of numerous separate burning events. In the drier south, fire scars are more likely to occur as large patches in a predominantly unburned landscape matrix. This pattern is evident in Namibia, Botswana, and along the border between South Africa and Mozambique. The spatial

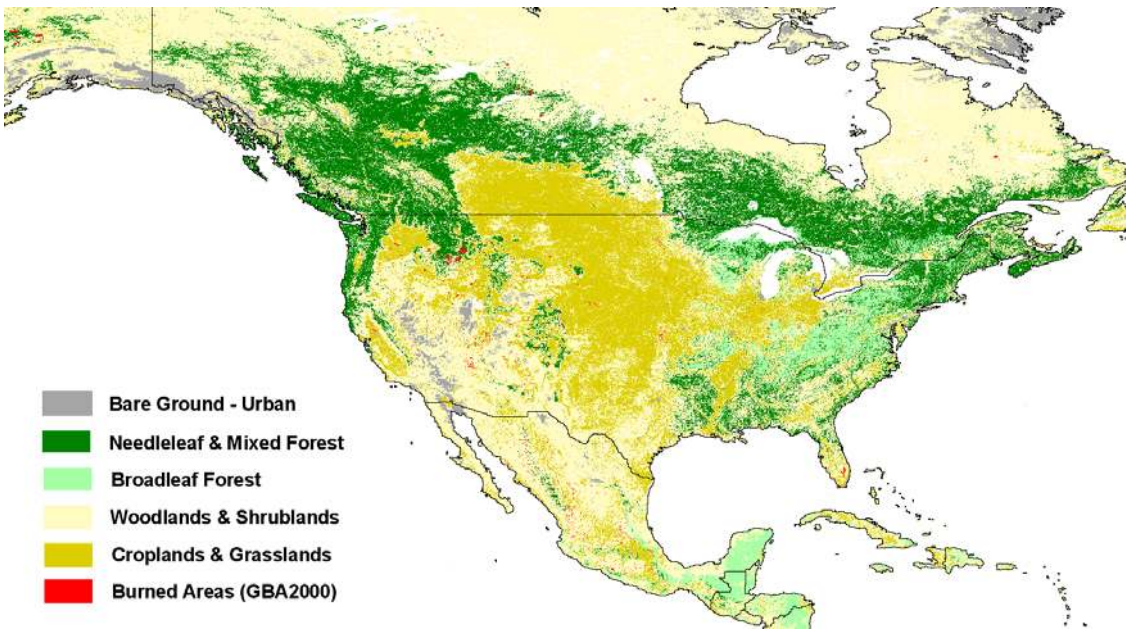

Figure 5. Burned area and grouped UMD vegetation map for North America in the year 2000 (scale 1:26,000,000).

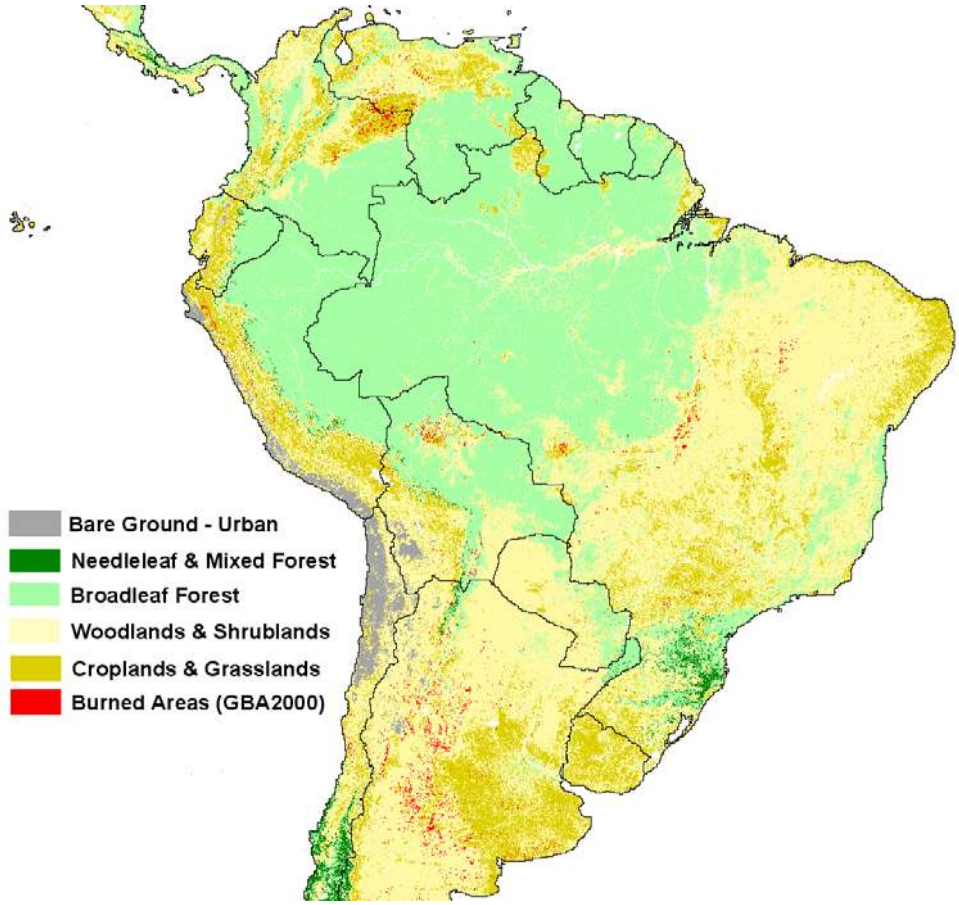

Figure 6. Burned area and grouped UMD vegetation map for South America in the year 2000 (scale 1:23,000,000).

and temporal pattern of fire occurrence corresponds very well to the findings of *Dwyer et al.* [2000], based on the analysis of 1-year of active fires data from the AVHRR and *Barbosa et al.* [1999], and is similar with the pattern of burning produced by *Silva et al.* [2003] for southern Africa. In DR Congo, Angola, Mozambique, Zambia, Tanzania, and South Africa, the vegetation class having the greatest burned area was the W&S class. The causes of burning in Africa are related to the clearing of natural vegetation for cultivation, the control of shrub encroachment on grazing lands, the promoting of nutrients cycling in pastures and croplands, and the driving of game for hunting. For Africa as a whole, small errors are present in the burned area products; these are mainly caused by flooding of nonpermanent water features and hot dark rocks in the east of Africa, but when compared with the magnitude of burning in Africa, these false detections are insignificant. In southern Africa, fire occurrences at the start of the rainy season may have been missed due to cloud cover. When compared to the GLOBSCAR product, the reported burned areas are always greater. For example, in Namibia the GLOBSCAR product only detects 7% of the area detected by GBA-2000, and in South Africa the area detected is three times as large. In Africa it is quite difficult to determine if the findings indicate average burning activity without producing similar products covering several years. Statistics for burned areas can be found for regions of South Africa and Namibia, but comparison data are not easily available for Mozambique, Madagascar, Zambia, Zimbabwe, Tanzania, and Angola (for more information, please refer to http://www.fire.uni-freiburg.de/iffn/country/country.htm).

4.2.2. Sub-Saharan Africa

[27] In the African continent (see Figure 1), from 18° north to the equator and 18° west to 55° east, burning activity has a significant presence in three broad types of vegetation dominating the region: BF, W&S, and G&C. The temporal distribution of fires, or fire seasonality, is almost the same for the three vegetation types. W&S and G&C mostly burn between November and February, coinciding with the Northern Hemisphere dry season, with a peak in December. In the case of BF the fire season starts in December and continues until March 2000, with a peak in January 2000 and a temporal shift being generally located more toward the south with respect to the other two vegetation classes. The extension of burned area in BF is still high in March owing to the contribution of dry forest burning in Ethiopia. An anomaly with respect to this general temporal trend is shown by forests situated in DR Congo, where fire activity is concentrated between July and November 2000, as it typically occurs in the Southern Hemisphere.

[28] Large differences are observed for the extension of burned areas in the different vegetation types. W&S is the class responsible for the majority of burned areas in the region with more than 1.1 million km^2 compared to G&C

where burned areas are one order less (0.11 million km^2). Burned areas in BF total 3780 km^2 for the year 2000. The largest component of burned areas is concentrated within a month of peak burning activity and contributes to about 40% of the total annual burned area for BF (1500 km^2) in January and W&S (450,000 km^2) in December and to about 30% for the G&C class (35,000 km^2) in December. Concerning the spatial distribution of burned areas, Ethiopia, Sudan, Central African Republic, Congo, and Cameroon are the five countries which mostly contribute to burned areas in BF, with 30, 25, 16, 14, and 12%, respectively. The Gabon does not contribute at all in the year 2000 with only 18 km^2 detected, even though it is almost entirely covered by forests and close to Congo and Cameroon. Forty per cent of all burned W&S areas are located in Sudan, Central African Republic, and Ethiopia, contributing 20, 10, and 10% each of the total burned area, respectively. The larger extensions of G&C burning can be found in the eastern part of the region with 33% in Ethiopia and 24% in Sudan. Ghana, Nigeria, and Sierra Leone in the west of the region contribute 10, 5, and 5% respectively. Estimates of burned areas are difficult to evaluate because of a lack of national data available for these countries. However, some broad values can be found, such as over 0.6 million km^2 burned annually in Sudan (for more information, refer to http://www.fire.uni-freiburg.de/iffn/country/sd/sd_1.htm) compared to a value of 0.4 million km^2 from GBA-2000 and for Ethiopia, a national statistic for forested areas is estimated at 950 km^2 (for more information, refer to http://www.fire.uni-freiburg.de/iffn/country/et/et_3.htm) compared to a value of 1033 km^2 from GBA-2000.

4.2.3. Southern Europe

[29] The countries that contributed most to the total area burned in southern Europe (see Figure 2) were Portugal, Spain, Italy, Greece, Hungary, Romania, and Bulgaria. In Portugal, Spain, and Greece the vegetation class with the largest estimate of burned area was W&S, whereas in Italy, Hungary, Romania, and Bulgaria this place is occupied by the G&C class. In southern Europe, most burning took place between June and October. For the southern European countries, estimates were compared with values derived from RESURS MSU-E A data [*San Miguel et al.*, 1998] for burn scars greater than 50 hectares. Estimates were compared in France with 549 km^2 (GBA-2000) compared to 151 km^2 (RESURS), Italy with 2521 km^2 (GBA-2000) compared to 451 km^2 (RESURS) and 595 km^2 (GBA-2000 without agriculture) compared to 956 km^2 (a national statistic estimated in 2000, not including agricultural fires, taken from http://www.fire.uni-freiburg.de/iffn/country/it/it_5.htm), and Greece with 1169 km^2 (GBA-2000) compared to 1017 km^2 (RESURS) and 1670 km^2 (a national statistic estimated in 2000 and taken from http://www.fire.uni-freiburg.de/iffn/country/gr/gr_14.htm).

[30] A detailed analysis was made for the Iberian Peninsula (Spain and Portugal). The total burned area in Iberian Peninsula in the year 2000 was estimated by the GBA-2000 data set at 2564 km^2. The estimate of the Portuguese Ministry of Agriculture and the Spanish Ministry of Environment was 3466 km^2; therefore an under-estimation was made by the GBA-2000 product of 30%. The estimate given by the RESURS study was 2198 km^2. One reason for this under-estimation is that, according to official statistics, during the month of March 2000, 9.3% of the total annual burned area of Portugal and 10.4% of the total annual burned area of Spain was consumed. Unfortunately, the burned area algorithms were not applied to satellite data in March 2000 to capture this unusual occurrence. The RESURS data set mapped only burned areas greater than 50 hectares, and these are thought to account for 73% of the total burned area each year in southern Mediterranean countries. The months having the most burning activity were August and September. The area burned in Portugal in July, August, and September accounts for almost 85% of the total burned area in the year 2000, as reported by the Portuguese Ministry of Agriculture. The spatial pattern of the GBA-2000 burned areas is very similar with the spatial pattern of the map produced for Portugal with Landsat TM imagery and also in Spain from the Spanish Ministry of the Environment. In the south of Portugal, commission errors are observed, caused by the application of a dual algorithm. At the regional scale the UMD global land cover map legend is not adequate for southern Europe. In Portugal and Spain, there are large areas of pine forest where the majority of fire activity is located; these regions are classified as W&S in the UMD product. It is understood that the burning activity throughout southern Europe in the year 2000 was close to the average reported for the last decade. Concerning the causes of fire, the Mediterranean basin is marked by a prevalence of human-induced fires [*Alexandrian et al.*, 1999] such as the burning of shrublands to create pastures, burning of crop residues, and arson. Determining the reliability of the products is difficult for Europe because often the burn scar is relatively small, and for small scale studies the authors urge care to be taken when using global land cover products to derive their products.

4.2.4. Russia

[31] In Russia (see Figures 2 and 3) the total estimated burned area in the year 2000 was approximately 222,000 km^2, of which 13% was N&MF, 41% W&S, and 46% G&C. These values compare to an estimate of 200,000 km^2 from the GLOBSCAR product. Both these products indicate values far greater than UN Food and Agricultural Organization (FAO) statistics of approximately 20,000 km^2. The main regions of grassland and cropland burning occurred in southern Russia, at the border with Kazakhstan, Mongolia, and China. Burning in these regions mainly occurred during April and May and again in September and October. The burned area estimated for N&MF for the year 2000 was $\approx$30,000 km^2. However, we do not state that this area corresponds to the amount of boreal forest consumed. The exact extent of Russian boreal forests is not generally known or easily determined; hence the burned area is only assumed for the merged classification of the UMD global land cover product (N&MF). It is difficult to compare estimates with national statistics that are available for land areas classified as forest fund, forest land, nonforest land, forested areas, and unforested areas (for more information, refer to http://www.fire.uni-freiburg.de/iffn/country/rus/rus_26.htm). In the boreal regions the interannual variation in burned area can be very large indeed, and this figure reflects only the area mapped in the year 2000. It is reported that burning activity in the year 2000 was not a particularly intense in the forested regions, when compared to 1998 for example. However, it may be possible that burning activity

in agricultural regions may occur on an annual basis and that estimates for this land cover type may not vary between years with any significance. In central and eastern Russia and northern Asia, it is understood that there are small areas of commissioned pixels in forested ecosystems and a small amount of omitted pixels in grassland ecosystems.

4.2.5. Mongolia and Northern China

[32] In Mongolia (see Figure 3), large burn scars are detected from April to June 2000, and in fact these fires occur within a few days of a thin snow cover melting. Some of the individual burned areas detected were truly huge. The total burned area in the year 2000 was estimated at $\approx$26,000 km^2, of which 64% lies within the G&C vegetation class. According to the statistics, 31% of total burned area was W&S, and the remaining 5% was N&MF. There were 1,647 scars detected in this class. Historically, it is thought that an average of 17,400 km^2 is burned every year, and more recently a value of 47,700 km^2 was estimated for a 10 year period between 1990 and 1999 (for more information, refer to http://www.fire.uni-freiburg.de/iffn/country/mn/mn_11.htm). Therefore it would appear that the year 2000 was more in keeping with average conditions based on historical information. The reason for burning in the early part of the year is thought to be due to the clearing of land for the generation of fresh grass used for grazing. Biomass burning in northern China (see Figure 3) occurs mostly between April and June. The percentage of the total area burned for each merged vegetation class is 46% for W&S, 37% for G&C, 14% for N&MF, and 3% for BF. Burning in the temperate forest of China mainly occurs in Heilongjiang Province and northern Inner Mongolia Province. The burned areas in this type of forest are small and dispersed. National statistics for a period between 1990 and 1999 indicate an average burned area of 1220 km^2 for forested areas (the comparable value for GBA-2000 is $\approx$10,500 km^2). However, there is considerable interannual variation in burned area (for more information, refer to http://www.fire.uni-freiburg.de/iffn/country/cn/cn_6.htm), but the evidence indicates that the burning activity in China was greater than on average. Agricultural burning, forestry, general carelessness, and lightning are the major ignition sources of wildfires after forest exploitation expanded by the mid-1960s.

4.2.6. India and Continental Southeast Asia

[33] The fire season in the Indian subcontinent and in continental southeast Asia (see Figure 3) is spread over the dry months of the Northern Hemisphere. The 1999–2000 fire season ended in May, and the 2000–2001 season started in October of that year. The peak of the activity is the period between March and May for India, while it is slightly earlier, February to April, in Myanmar, Cambodia, Laos, Vietnam, and Thailand. In India the fire activity is mainly concentrated in the W&S class; in the year 2000, more than 43,000 km^2 (about 90% of the total burned area) burned in this vegetation class. Another 3300 km^2 burned in the G&C class (7% of the total burned area), and about 400 km^2 burned in the forest classes. Data from national statistics vary by a considerable amount. Two sources of information estimate that an annual average of forest loss is between 14,500 km^2 and 37,300 km^2 each year (for more information, refer to http://www.fire.uni-freiburg.de/iffn/country/in/in_5.htm). Given that some of the area defined as forests is included in the W&S class, it would indicate that the burning activity in India in the year 2000 was close to average conditions. The burning activity affects about 1.6% of the total surface of the country. It is interesting that burning activity observed in India is significantly lower than that indicated by active fire products, e.g., the ATSR-2 World Fire Atlas (http://odisseo.esrin.esa.it/ionia/FIRE/AF/ATSR/) and the Global Fire Product (http://www.fire.uni-freiburg.de/iffn/research/res_1.htm). Confirmation of these false detections in the active fire products was confirmed through observations of Landsat TM quick-look data products. In Myanmar, Cambodia, Laos, Vietnam, and Thailand the predominant vegetation is W&S, followed by G&C. In Myanmar, Cambodia, Laos, and Vietnam the fire activity, like in India, affects mainly W&S areas, while in Thailand burning affects mainly G&C. Myanmar has more than 11,000 km^2 of burned area, and along with Cambodia with 3900 km^2, they make the largest contribution to the total amount of land burned in the region. Thailand follows with about 2000 km^2 of burned area, then Laos with 1450 km^2, and finally Vietnam with 350 km^2. With the exception of Myanmar, where fire affects 1.5% of the territory, only about 0.5% of the whole region is affected by fire. In Thailand the GLOBSCAR product estimates three times the area burned in the year 2000, a national statistic estimate for forests burned in the year 2000 is 933 km^2 (for more information, refer to http://www.fire.uni-freiburg.de/iffn/country/th/th_2.htm), close to the GBA-2000 estimate for W&S at 929 km^2.

4.2.7. Insular Southeast Asia

[34] The areas burned in each vegetation class in the three main countries of insular southeast Asia (see Figures 3 and 4), Indonesia, Malaysia, and Papua New Guinea (here included in the reporting for southeast Asia) were 63% W&S, 28% G&C, and 8% BF for Indonesia; 44% G&C, 28% W&S, and 26% BF for Sarawak province of Malaysia; and 56% W&S, 25% BF, and 18% G&C for Papua New Guinea. The total area burned in these countries is very small, only 2043 km^2, and therefore the corresponding burned areas in the tropical forest are also very small. No clear spatial pattern of burning in this tropical forest is observed, but this is typical of tropical forest burning in any part of the world. The sources of the fire are mostly anthropogenic and are largely influenced by climatic conditions triggered by El Niño and La Niña events and therefore can vary significantly from year to year. For example, during the El Niño event of 1997–1998, national statistics provided an estimate of the total burned area in Indonesia of approximately 97,000 km^2 (for more information, refer to http://www.fire.uni-freiburg.de/iffn/country/id/id_35.htm). During the La Niña event of the year 2000, only 1880 km^2 were detected as being burned in the GBA-2000 product. This would indicate that the year 2000 was on average a low fire activity year in Indonesia. This statement can be assumed to represent the situation in insular southeast Asia (Malaysia and Papua New Guinea). Some of the major reasons why fires are set are for the preparation of land to establish agricultural plantations, shifting cultivation by indigenous peoples, camping and natural causes such as lightning. In a lot of cases, controlled fires set for the establishment of agricultural plantations or for the clearing of land prior to planting are not well managed and quickly

become out of control and spread into the surrounding vegetation. Owing to persistent cloud cover in insular southeast Asia and the relatively small size of burn scars in tropical forests, it is likely that an under-estimation of the true burned area in this region has been made.

4.2.8. Australia

[35] In Australia (see Figure 4), 94% of the area mapped as burned in 2000 occurred in the W&S class, 5% in the G&C class, and 1% in the remaining forest classes (N&MF and BF). These statistics confirm that fires in Australia are mainly savanna fires. The largest and most frequent fires in the whole country occur in the tropical savanna ecosystems in northern Australia, where Sorghum sp. grasses have become established during the wet season, support large fires. The area burned amounted to almost 8% of the total area of W&S in Australia. Fires are less frequent in southern Australia, although they can be more intense and severe because of their impact on human health and society. Severe fires occurred in forests during the Southern Hemisphere summer months in 2001 and 2002 near Sydney. In these ecosystems the return period of fire is counted in tens of years and decomposition allow for surface as well as canopy fuel loads to build up, thus creating a potentially dangerous environment. High fuel loads often support intense crown fires that can spread with high speed through the canopy. Despite the area burned in forests being small, it still represents 1.7% of the total area of N&MF and 1.7% of BF in Australia.

[36] The total area estimated by the GBA-2000 product was approximately 0.56 million km^2. It is thought that there is an under-estimation of the true burned area in Australia when compared to an official national statistic of 0.7 million km^2 from the Western Australia Department of Land Administration (DOLA). The same national assessment undertaken the year before estimated 0.31 million km^2 burned (for more information, refer to http://www.fire.uni-freiburg.de/iffn/country/au/au_8.htm). The estimate from the GLOBSCAR product was 0.18 million km^2. The under-estimation made by GBA-2000 is believed to be due to burning activity occurring in sparse, Spinifex sp. grasses growing in bright, red sand soils (D. Graetz, CSIRO, personal communication, 2002). Fires in this type of vegetation cause the surface to increase in reflectance, the opposite of what occurs in other vegetation types, and this makes detection of these burned areas using the current algorithms very difficult. Burning activity is heavily controlled and managed in Australia, with many prescribed fires occurring in the early dry season that limits the buildup of biomass. However, very large fires occur toward the end of the dry season in the northern tropical savanna region. Lightning and fires set either accidentally or deliberately are also common causes of fire in Australia. Given such variation in the burned area reported for Australia, it is difficult to assess whether the year 2000 burned area estimates were typical of average burned areas and the impact of large-scale climatic events such as El Niño and La Niña events have on burning activity in the country.

4.2.9. United States of America and Canada

[37] In the USA (see Figure 5) the burning activity was concentrated in April through September with small occurrences of activity through the Northern Hemisphere winter months in some southern States. Fire incidence was higher in the western third of the country, mainly in Idaho, Washington, Oregon, Montana, Wyoming, and Alaska. The total burned area in the USA in the year 2000 was estimated at ≈35,000 km^2, which is only around 4% bigger than the value of 33,689 km^2 given by the National Interagency Fire Center. The year 2000 was reported to be one of the worst wildfire years for over fifty years, in excess of average estimates of burned area (for more information, refer to http://www.fire.uni-freiburg.de/iffn/country/us/us_17.htm). Concerning the relationship between vegetation and burning, 50% of the area burned in the year 2000 occurred in the W&S class, 33% in the G&C class, and 17% in the N&MF class. Concerning the causes of vegetation fires, debris burning, campfires, arson, use of equipment, and lightning are common. In fact, the forests fires that occurred in the western United States during the year 2000 were well documented as they were particularly large and devastating. The reason for the increased burning activity in the US forests in the year 2000 may be attributable to large-scale climatic phenomena such as El Niño and La Niña, which describe the condition of the ocean-atmosphere system in the tropical Pacific Ocean. This state of the climate cycle results in elevated temperatures and changes in humidity and can have a large impact on the severity and distribution of vegetation burning at a global scale, as was observed in 1997 in Indonesia during an El Niño event [*Siegert et al.*, 2001]. During the summer of 2000 it is understood that hotter dryer conditions existed over the western United States resulting in devastating fires. In North and Central America, there may be some false detections in the semiarid regions of the US and Mexico, but this has not been confirmed. In parts of Mexico the detection of burned areas from satellite data is hindered by cloud cover and the fact that burned areas in this region tend to be small.

[38] In Canada (see Figure 5) the estimated area burned in the year 2000 was 5560 km^2, of which 28% was N&MF and 68% W&S. According to *Fraser et al.* [2003], the area falsely mapped in Canada was 3.5% and most burn scars over 10 km^2 were mapped with high confidence. A number of small burn scars were not detected by the algorithm. However, burned areas less than 10 km^2 were found to contribute only 2.4% of the total burned area in Canada during 1998. When compared to the burned area estimate from the Canadian Interagency Forest Fire Center (CIFFC), the estimate derived from the GBA-2000 project was 3% smaller. Compared to the CIFFC burned areas estimates for 1998 (47,108 km^2) and 1999 (17,056 km^2), the burned area estimated in the year 2000 was much smaller (12% of 1998 and 33% of 1999) and was one of the lowest years for fire activity recorded in the past few decades. A reason for this smaller than average fire year may be the climate caused a forcing of wetter weather further north in the year 2000. Canada also experiences a large interannual variation as documented by *Amiro et al.* [2001] and *Stocks et al.* [2002].

4.2.10. Brazil

[39] Brazil (see Figure 6) is characterized by different types of vegetation such as tropical rain forest, evergreen forest in the northeast, savanna (called Cerrado locally) in the central part of the country, and temperate rain forests

along the coast in the east (Mata Atlantica). The regions of Brazil with the greatest burning activity are Mato Grosso, Pará, Tocantins, Maranhão, Piauí, Bahia, Goiás, Minas Gerais, and Mato Grosso do Sul. The vegetation type affected by fire in Brazil is mainly the Cerrado, a savanna of grassland, and woodland. Most burned areas in this vegetation type were detected between June and August 2000, corresponding to the dry season and between September and October 2000, corresponding to the arrival of the rains [*Goldammer*, 1990]. The vegetation classes W&S and G&C contribute 67 and 29%, respectively, to the total area burned in the year 2000. The area burned in the BF class is only 5% of the total burned area in Brazil. Compared to the GLOBSCAR product that reported 4333 km^2 of forest burned, the GBA-2000 product reported only 846 km^2, 80% less. However, it is difficult to confirm if detections of flooded areas has contributed to the GLOBSCAR estimate. For the whole of Brazil, GLOBSCAR estimates were three times larger. There are even more detections reported from the ATSR-2 World Fire Atlas products, but it cannot be assumed that every active fire contributes a burned area of 1 km^2; hence these values cannot be directly compared. Obtaining estimates for comparison from national statistics is quite difficult because of the diverse nature of vegetation in Brazil, differences in statistical reporting, and reliability of information (for more information, refer to http://www.fire.uni-freiburg.de/iffn/country/country.htm#BRAZIL). The fires in the Cerrado are predominantly caused by farmers. They use fire during the dry season to promote the growth of fresh grass in pastures for their cattle and to clear fields to make them ready for cultivation in the wet season [*Coutinho*, 1990]. There are still some burning activity caused by implementing pest control measures and carelessness in areas of controlled burning, such as during the cutting and burning of vegetation while clearing the edges of highways and railroads [*Goldammer*, 1990]. It is clear that the GBA-2000 product does not clearly detect the ''arc of deforestation'' in the southern Amazon region, between 200 and 600 km in width and approximately 3000 km in length extending from the State of Maranhão in the east through parts of Tocantins, Pará, Mato Grosso, Amazonas, Rondônia, and Acre in the west. This is because we cannot easily distinguish whether the burned areas detected are related directly to deforestation. Burned areas are detected within this broad arc but mainly outside of the forest as defined by the UMD product. Burn scars are detected in central parts of eastern Brazil, but no major patterns of detections occur along this arc. There are a number of explanations for not clearly detecting burn scars within this arc at the edges of the forest. The area of deforestation may be smaller than 1 km^2 and therefore difficult to detect with the sensor used in this study. Ground fires may not be detected at all, as the spectral characteristics of the canopy will not be altered. Cloud cover obviously plays a significant role in obtaining a clear observation of the ground surface in humid tropical regions. Hence it is clear that there are limitations to the accurate determination of burned area in this region. The year 2000 was a La Niña year characterized by unusually cool temperatures in the equatorial Pacific Ocean, and this may be the reason why we observe a mild fire season, compared to annual statistics, in Brazil and also in Indonesia. With reference to the paper by *Fearnside* [2000], it is difficult to detect burning activity of secondary land cover mainly because of the fact that the product discussed in this paper is related to the year 2000 only, and detection of the same area burned twice is not possible within this timeframe.

4.3. Monthly Burned Area Estimates in the Central African Republic

[40] Information on annual burned area is not always sufficient to satisfy the data or modeling requirements of a number of research fields, including emission modeling and aerosol transport. Burned area estimates are required at a greater temporal resolution, such as on a daily or monthly basis. A daily product has not yet been realized, but the GBA-2000 data set provides monthly estimates. The Central African Republic (CAR) is a country of some 622,000 km^2 located approximately between 2° and 9° north and 15° and 27° east in sub-Saharan Africa. Burning in the CAR is undertaken for a number of reasons, including burning for land clearance for agriculture, hunting, national park management, and use of wood for fuel. Information on the timing of fires in the different types of vegetation in the CAR is important because emissions, biomass loading, fire severity, and combustion efficiency can vary considerably within a woodland and shrubland environment. In addition, from a land manager's point of view, the implementation of controlled burning at the beginning of the dry season is optimal because biomass levels are relatively low and fires are more easily controlled. Furthermore, there is a strong gradient of land cover types within the CAR and also interesting physical landforms such as the Bongo Massif, a high plateau in the south central part of the country.

[41] The area of each grouped vegetation class in the CAR is estimated to be approximately 35,000 km^2 for BF, 578,000 km^2 for W&S, and 5464 km^2 for G&C. Compared to the GLOBSCAR estimate of 97,272 km^2, the GBA-2000 detects more than twice the area burned, including pixels detected twice in the year 2000. The GBA-2000 estimates were also compared with values derived from the 1996 Experiment for Regional Sources and Sinks of Oxidants (EXPRESSO) experiment reported in the work of *Pereira et al.* [1999], 525,820 km^2 for burn scars, and 112,578 km^2 for active fire detections. However, the reader needs to be aware that only one-third of the dry season was studied, the area studied covered the CAR and parts of neighboring countries (Cameroon, Sudan, Chad, Nigeria, DR Congo) and the differences between the physical parameter detected by the active fire and burn scar algorithms. The main burning season in the CAR corresponds with the Northern Hemisphere dry season, normally commencing in late October or November, progressing south, and finishing in March. Therefore the year 2000 characterizes middle to late season burning in January to April 2000 and early season burning in October to November 2000. Figure 7 shows the spatial and temporal distribution of burning in the CAR in three time stages: January and February 2000, March and April 2000, and November and December 2000. Burning activity can clearly be seen progressing from north to south as the fire season develops between the months of

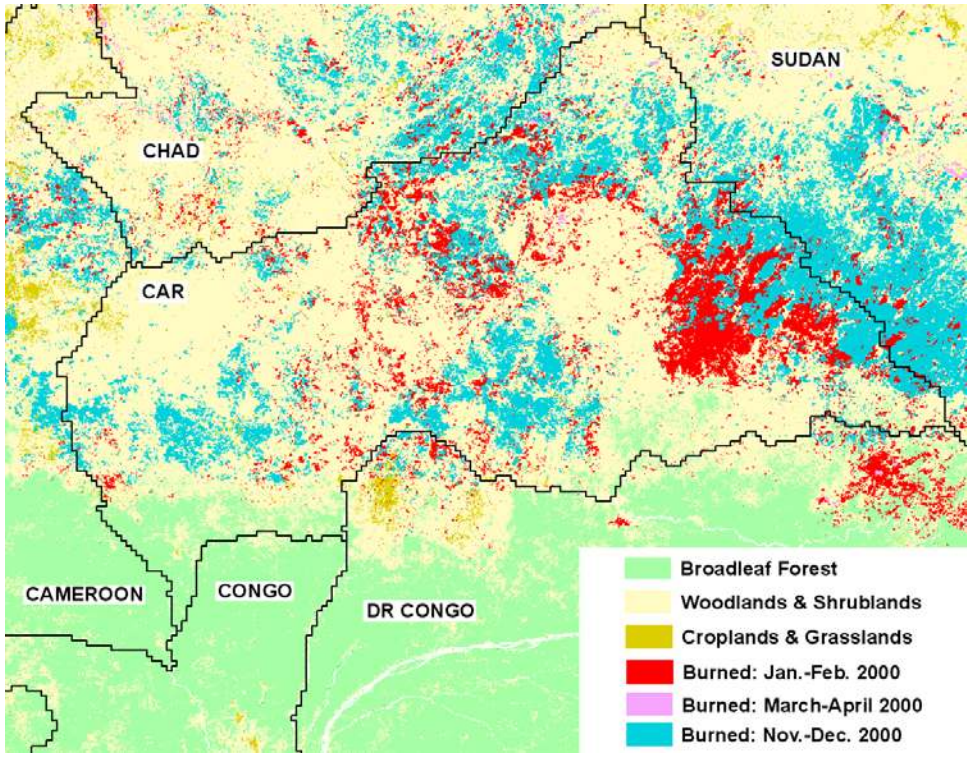

Figure 7. Burned area and grouped UMD vegetation map for the Central African Republic (CAR) in the year 2000 (scale 1:5,000,000). Burned areas are shown for three time periods, January-February 2000, March-April 2000 and November-December 2000.

November and April. It is clear that there is intense burning activity around the Bongo Massif and less intensive activity within the region. Of interest is that some activity is recorded in the late season (March and April) on the plateau. In the CAR it is also possible that areas can be burned twice, late in the 1999–2000 dry season and early in the 2000–2001 dry season. The burning of the same area twice in the year 2000 can be clearly seen in the estimates of monthly and annual burned areas for the CAR in Table 3. Table 3 shows monthly burned area estimates, the sum of the monthly burned areas, and the estimate of the actual area in the CAR burned in the year 2000. In the W&S class the sum of the monthly burned area estimates is approximately 213,000 km^2, of which just over 30,000 km^2 has burned twice in the year 2000. This can be compared to a value, considered to be an average fire season estimate, presented by *Eva and Lambin* [1998] of 277,000 km^2 for two types of savannah. During January and December 2000 the middle of the dry season, 90% of the total area burned. Toward the end of the dry season, in February and March 2000, 8543 km^2 and 1183 km^2 of burned areas, respectively, were detected in the W&S class. In the BF and G&C classes, 94 and 90%, respectively, of the total burned area occurred in January and December 2000. For more information related to the fire situation in the CAR, refer to http://www.fire.uni-freiburg.de/iffn/country/car/car_1.htm. In the example shown, a global land cover map has been used to derive the statistics. However, the use of the GBA-2000 data set is encouraged with regional land cover maps to provide a clearer understanding of the sensitivity of timing and location of burning activity to the local requirements of controlled burning and the impact on the vegetation.

4.4. Validation Issues

[42] A global validation of the GBA-2000 product is not available at this time. Work is currently being undertaken

Table 3. Monthly Burned Area Estimates (km^2) for the Central African Republic for the Year 2000[a]

Vegetation Class	Jan.	Feb.	March	April	May	Oct.	Nov.	Dec.	Sum 2000	Year 2000	Class Burned, %
Broadleaf forest	369	32	6	0	0	0	0	207	614	529	1.5
Woodlands and shrublands	94479	8543	1183	196	27	70	11126	97305	212929	182832	31.6
Grasslands and croplands	542	52	36	5	2	0	117	1267	2020	1813	33.2

[a]The column labeled "Sum 2000" indicates the sum of the monthly area estimates in the year 2000. The column labeled "Year 2000" indicates the estimated physical area burned at least once in the year 2000. The difference between these two values is the area detected as being burned twice. June to September are not shown as this corresponds to the wet season in this region. Small differences occur between these figures and those shown in Table 2 because of resampling the global product to an equal area projection.

to derive a suitable sampling strategy that will enable a regionalized validation to be made. However, the validation exercise is limited by human resources and the availability and cost of Landsat TM imagery (30 m pixel size satellite data) used for the validation. Techniques and methods that are being considered in assessing the accuracy of the end-product are outlined by *Boschetti et al.* [2001] and include the use of correlation analysis to assess surface area accuracy, overall map, producers and users accuracy's, and the map's 1 km accuracy. For each of the regional algorithms a performance indicator is presented in the work of *Grégoire et al.* [2003], derived using selected Landsat TM scenes over the corresponding region of interest.

5. Conclusions

[43] An inventory of the extent of global biomass burning for four broad vegetation groups in the year 2000 is described in this paper, with reference to the location and characteristics of the burned areas. An example is presented on the use of monthly estimates of burned area at the country level as an aid to monitoring and managing the burning of vegetation. The global burned area products, developed under the GBA-2000 initiative [*Grégoire et al.*, 2003], are available to the user community, free of charge at http://www.gvm.jrc.it/fire/gba2000/index.htm. The results (maps) can be viewed through the UNEP Web site at http://www.grid.unep.ch/activities/earlywarning/preview/ims/gba/ indicate for the first time the global spatial and temporal distribution of burned area scars at a detection resolution of approximately 1 km^2 for the year 2000. The maps show the extent of agricultural land burning in southern Russia, large areas of burning activity in northeastern China and eastern Mongolia shortly after the snows have melted in April, the seasonality of burning activity is sub-Saharan Africa, the effects of devastating forest fires in western USA and very little activity detected in Canada, and many other interesting observations worthy of further investigation. The results also indicated the problems of remote sensing approaches for detecting burned areas in cloudy regions, detecting burned areas smaller than the resolution of the sensing instrument (a significant problem in regions of tropical forest), and the false detection of burned areas caused by flooding or dark rocks.

[44] The information presented in this paper provides spatial and temporal estimates of vegetation burning for four merged vegetation classes derived from University of Maryland (UMD) global 1 km land cover product at the global scale and provides the research community with direct estimates of one of the most uncertain parameters in the calculation of total biomass consumed by fire and gas emissions resulting from vegetation fires [*Levine*, 1996]. Knowing the area burned will help constrain the uncertainties involved in modeling the response and feedbacks of the climate and vegetation system to climate change. The products can help to reduce uncertainties in estimates of biomass consumed and emissions because the data are available on a monthly basis and not just a single yearly estimate. If emission models being used by the community have a temporal component, then monthly data can be used. Uncertainties are also reduced because the data are available at a resolution of 1 km^2 at the global scale, suited for regional, continental, and global studies. Finally, a validation experiment is underway to provide more confidence in the estimates presented in this paper. The validation will focus on two regions, Africa and Eurasia, and will utilize Landsat Thematic Mapper data. Results of this exercise are expected in early 2004. The products can also be used with other land cover data sets, e.g., with the global croplands data set [*Ramankutty and Foley*, 1998], to provide an insight into burning of agricultural areas. Having at least one other global burned area product available to the scientific community (GLOBSCAR), users can test the sensitivity of their biomass or emission models to the estimation of burned areas. The year 2000 was chosen as the year to conduct this experiment because of the availability of satellite data giving global daily coverage. However, it has been shown in the literature that there is significant multiannual variation in the spatial distribution and also in the timing of vegetation fires [*Duncan et al.*, 2003]. The causes of these fluctuations are mainly driven by climatic factors such as temperature, precipitation, and humidity or large-scale climatic phenomena such as El Niño and La Niña. They may also be caused by changes in the management or use of the land. The burned area estimates, presented in this paper, should be used with caution if the user intends to use the data to describe mean conditions or make extrapolations to other years. However, the intention of this paper is to provide reference information and estimates of burned area for comparison with for future estimates. In order to make predictions, multiannual estimates are required for several years including El Niño and La Niña events. In the short term the methodology and a number of algorithms developed in the context of the GBA-2000 initiative will be used in the implementation of the GLOBCARBON project of the European Space Agency, providing global, monthly, burned area products over 5 years (1999–2003).

[45] The amount of biomass burning and gas emissions is also a political issue within the context of the Framework Convention of Climate Change and the Kyoto Protocol. The results in this paper indicate potential focus areas where biomass burning is contributing a significant amount to sources of greenhouse gases, e.g., in developing countries in Africa. The GBA-2000 product can contribute to updating biomass burning and emission inventories, and work is underway to incorporate the findings of the study into the EDGAR database (for more information, refer to http://arch.rivm.nl/env/int/coredata/edgar/index.html). It has been shown that a large proportion of burning activity takes place within the tropics. It is important in atmospheric chemistry to know the contribution of gas release to the lower, middle, and upper troposphere, and strong vertical fluxes in these regions [*Andreae and Merlet*, 2001] will have an impact on the chemical composition of the atmosphere at the global scale. Equally important is the detection of fires in the temperate and boreal zones that represent large pools of organic carbon (that take a long while to return after a fire event) and the fact that this product has shown to achieve with some success particularly in the US and Canada. This information will enable modelers of atmo-

spheric and terrestrial chemistry to study the uptake of carbon and other gases in these regions and at the global scale.

[46] Future work will concentrate on validation issues, as mentioned previously. In addition, the regional algorithm approach to global mapping has yielded several new methods for burned area mapping, including the use of neural networks. The approach has also indicated how algorithms may be improved in the future by combining the best components of several algorithms. An algorithm that yields burned areas on a daily basis at the global scale has been developed and is currently processing the year 2000 image data set. Finally, we hope to calculate estimates of the biomass burned and gas emissions using the GBA-2000 products. Biomass loading will be derived from the Global Land Cover (GLC) 2000 product, the latest global land cover product to be released [*Bartholomé et al.*, 2002], and emissions will be calculated using published methods and emission factors.

References

Alexandrian, D., F. Esnauld, and G. Calabri (1999), Forest fires in the Mediterranean area, *Unasylva*, *197*, 35–41.

Amiro, B. D., J. B. Todd, B. M. Wotton, K. A. Logan, M. D. Flannigan, B. J. Stocks, J. A. Mason, D. L. Martell, and K. G. Hirsch (2001), Direct carbon emissions from Canadian forest fires 1995–1999, *Can. J. Forest Res.*, *31*, 512–525.

Andreae, M. O. (1997), Emissions of trace gases and aerosols from southern African savanna fires, in *Fire in Southern African Savannas: Ecological and Atmospheric Perspectives*, edited by B. W. van Wilgen et al., pp. 161–184, Witwatersrand Univ. Press, Johannesburg.

Andreae, M. O., and P. Merlet (2001), Emission of trace gases and aerosols from biomass burning, *Global Biogeochem. Cycles*, *15*, 955–966.

Andreae, M. O., E. Atlas, H. Cachier, W. R. Cofer III, G. W. Harris, G. Helas, R. Koppmann, J.-P. Lacaux, and D. E. Ward (1996), Trace gas and aerosol emissions from savanna fires, in *Biomass Burning and Global Change*, edited by J. S. Levine, pp. 278–295, MIT Press, Cambridge, Mass.

Barbosa, P. M., D. Stroppiana, J.-M. Grégoire, and J. M. C. Pereira (1999), An assessment of vegetation fire in Africa (1981–1991), Burned areas, burned biomass, and atmospheric emissions, *Global Biogeochem. Cycles*, *13*, 933–950.

Bartholomé, E., A. S. Belward, F. Achard, S. Bartalev, C. Carmona-Moreno, H. Eva, S. Fritz, J.-M. Grégoire, P. Mayaux, and H.-J. Stibig (2002), GLC2000—Global land cover mapping for the year 2000, project status November 2002, *Publ. EUR 20524 EN, Eur. Commun.*, Brussels.

Boschetti, L. (2003), A multitemporal algorithm for burned area detection in Mexican woodland and shrubland environment with SPOT-VEGETATION data, in *Proceedings of the 2003 IEEE International Geoscience and Remote Sensing Symposium*, vol. II, pp. 1293–1295, IEEE, New York.

Boschetti, L., S. Flasse, S. Trigg, P. A. Brivio, and M. Maggi (2001), A methodology for the validation of low resolution remotely sensed data products, in *Proceedings of the 5th ASITA Conference*, pp. 293–298, ASITA, Rimini, Italy.

Boschetti, L., S. Flasse, S. Trigg, and A. J. de Dixmude (2002), A multitemporal change detection algorithm for the monitoring of burnt areas with Spot Vegetation data, in *Analysis of MultiTemporal Remote Sensing Images*, edited by L. Bruzzone and P. Smits, pp. 75–82, World Sci., Tokyo.

Breiman, L., J. H. Friedman, R. A. Olshen, and C. J. Stone (1984), *Classification and Regression Trees*, Wadsworth, Belmont, Calif.

Brivio, P. A., M. Maggi, E. Binaghi, I. Gallo, and J.-M. Grégoire (2002), Exploiting spatial and temporal information for extracting burned areas from time series of SPOT-VGT data, in *Analysis of Multitemporal Remote Sensing Images*, edited by L. Bruzzone and P. Smits, pp. 132–139, World Sci., Tokyo.

Cabral, A., M. J. P. de Vasconcelos, J. M. C. Pereira, E. Bartholomé, and P. Mayaux (2003), Multitemporal compositing approaches for SPOT-4 VEGETATION, *Int. J. Remote Sens.*, *24*, 3343–3350.

Cahoon, D. R., B. J. Stocks, J. S. Levine, W. R. Cofer III, and K. O'Neil (1992), Seasonal distribution of African savannah fires, *Nature*, *359*, 812.

Cofer, W. R., III, J. S. Levine, E. L. Winstead, D. R. Cahoon, D. I. Sebacher, J. P. Pinto, and B. J. Stocks (1996), Source composition of trace gases released during African savanna fires, *J. Geophys. Res.*, *101*(D19), 23,597–23,602.

Colby, J. D. (1991), Topographic normalization in rugged terrain, *Photogramm. Eng. Remote Sens.*, *57*, 531–537.

Conard, S. G., A. I. Sukhinin, B. J. Stocks, D. R. Cahoon, E. P. Davidenko, and G. A. Ivanova (2002), Determining effects of area burned and fire severity on carbon cycling and emissions in Siberia, *Clim. Change*, *55*, 197–211.

Coutinho, L. M. (1990), Fire in the ecology of the Brazilian cerrado, in *Fire in the Tropical Biota: Ecosystem Processes and Global Challenges*, edited by J. G. Goldammer, pp. 82–105, Springer-Verlag, New York.

DeFries, R., M. Hansen, J. R. G. Townshend, and R. Sohlberg (1998), Global land cover classifications at 8 km spatial resolution: The use of training data derived from Landsat imagery in decision tree classifiers, *Int. J. Remote Sens.*, *19*, 3141–3168.

Delmas, R. A., P. Loudjani, A. Podaire, and J. C. Menaut (1991), Biomass burning in Africa: An assessment of annually burned biomass, in *Global Biomass Burning: Atmospheric, Climatic, and Biospheric Implications*, edited by J. S. Levine, pp. 126–132, MIT Press, Cambridge, Mass.

Duncan, B. N., R. V. Martin, A. C. Staudt, R. Yevich, and J. A. Logan (2003), Interannual and seasonal variability of biomass burning emissions constrained by satellite observations, *J. Geophys. Res.*, *108*(D2), 4100, doi:10.1029/2002JD002378.

Dwyer, E., J.-M. Grégoire, and J. P. Malingreau (1998), A global analysis of vegetation fires using satellite images: Spatial and temporal dynamics, *Ambio*, *27*, 175–181.

Dwyer, E., J. M. C. Pereira, J.-M. Grégoire, and C. C. DaCamara (1999), Characterization of the spatio-temporal patterns of global fire activity using satellite imagery for the period April 1992 to March 1993, *J. Biogeogr.*, *27*, 57–69.

Dwyer, E., S. Pinnock, J.-M. Grégoire, and J. M. C. Pereira (2000), Global spatial and temporal distribution of vegetation fire as determined from satellite observations, *Int. J. Remote Sens.*, *21*, 1289–1302.

Eastwood, J. A., S. E. Plummer, B. K. Wyatt, and B. J. Stocks (1998), The potential of SPOT-Vegetation data for fire scar detection in boreal forests, *Int. J. Remote Sens.*, *19*, 3681–3687.

Ershov, D. V., and V. P. Novik (2001), Mapping burned areas in Russia with SPOT4 VEGETATION (S1 product) imagery, final report, *Contract 18176-2001-07-F1EI ISP RU*, Eur. Comm. Joint Res. Cent., Brussels.

Eva, H. D., and E. F. Lambin (1998), Burnt area mapping in central Africa using ATSR data, *Int. J. Remote Sens.*, *19*, 3473–3497.

Fearnside, P. M. (2000), Global warming and tropical land-use change: Greenhouse gas emissions from biomass burning, decomposition and soils in forest conversion, shifting cultivation and secondary vegetation, *Clim. Change*, *46*, 115–158.

Ferek, R. J., J. S. Reid, P. V. Hobbs, D. R. Blake, and C. Liousse (1998), Emission factors of hydrocarbons, halocarbons, trace gases and particles from biomass burning in Brazil, *J. Geophys. Res.*, *103*(D24), 32,107–32,118.

Food and Agriculture Organization of the United Nations (FAO) (2001), Global forest fire assessment 1990–2000, *Forest Resour. Assess. Prog. Working Pap. 55*, Rome.

Fraser, R. H., and Z. Li (2002), Estimating fire-related parameters in boreal forest using SPOT VEGETATION, *Remote Sens. Environ.*, *82*, 95–110.

Fraser, R. H., R. Fernandes, and R. Latifovic (2003), Multi-temporal mapping of burned forest over Canada using satellite-based change metrics, *Geocarto Int.*, *18*, 37–48.

Goldammer, J. G. (1990), *Fire in the Tropical Biota: Ecosystem Processes and Global Challenges*, Spring-Verlag, New York.

Govaerts, Y. M., J. M. Pereira, B. Pinty, and B. Mota (2002), Impact of fires on surface albedo dynamics over the African continent, *J. Geophys. Res.*, *107*(D22), 4629, doi:10.1029/2002JD002388.

Granier, C., J.-F. Muller, and G. Brasseur (2000), The impact of biomass burning on the global budget of ozone and ozone precursors, in *Biomass Burning and Its Inter-Relationships With the Climate System*, edited by J. L. Innes, M. Beniston, and M. M. Verstraete, pp. 69–85, Kluwer Acad., New York.

Grégoire, J.-M., K. Tansey, and J. M. N. Silva (2003), The GBA-2000 initiative: Developing a global burned area database from SPOT-VEGETATION imagery, *Int. J. Remote Sens.*, *24*, 1369–1376.

Hansen, M. C., R. S. Defries, J. R. G. Townshend, and R. Sohlberg (2000), Global land cover classification at 1 km spatial resolution using a classification tree approach, *Int. J. Remote Sens.*, *21*, 1331–1364.

Hao, W. M., and D. E. Ward (1993), Methane production from global biomass burning, *J. Geophys. Res.*, *98*(D11), 20,657–20,661.

Hastings, D. A., and P. K. Dunbar (1998), Development and assessment of the global land one-km base elevation digital elevation model (GLOBE), *Int. Soc. Photogramm. Remote Sens. Arch.*, *32*, 218–221.

Hoelzemann, J. J., M. G. Schultz, G. P. Brasseur, C. Granier, and M. Simon (2004), Global Wildland Fire Emission Model (GWEM): Evaluating the use of global area burnt satellite data, *J. Geophys. Res.*, *109*, D14S04, doi: 10.1029/2003JD003666.

Hoffa, E. A., D. E. Ward, W. M. Hao, R. A. Susott, and R. H. Wakimoto (1999), Seasonality of carbon emissions from biomass burning in a Zambian savanna, *J. Geophys. Res.*, *104*(D11), 13,841–13,853.

Isaev, A. S., G. N. Korovin, S. A. Bartalev, D. V. Ershov, A. Janetos, E. S. Kasischke, H. H. Shugart, N. H. F. French, B. E. Orlick, and T. L. Murphy (2002), Using remote sensing to assess Russian forest fire carbon emissions, *Clim. Change*, *55*, 235–249.

Johnson, R. A., and D. W. Wichern (1988), *Applied Multivariate Statistical* Analysis, 2nd ed., Prentice Hall, Old Tappan, N. J.

Kasischke, E. S., N. L. Christensen Jr., and B. J. Stocks (1995), Fire, global warming, and the carbon balance of boreal forests, *Ecol. Appl.*, *5*, 437–451.

Kaufman, Y. J., A. Setzer, D. Ward, D. Tanré, B. Holben, P. Menzel, M. Pereira, and R. Rasmussen (1992), Biomass burning airborne and spaceborne experiment in the Amazonas (BASE-A), *J. Geophys. Res.*, *97*(D13), 14,581–14,599.

Kaufman, Y. J., D. Tanré, and O. Boucher (2002), A satellite view of aerosols in the climate system, *Nature*, *419*, 215–223.

Kempeneers, P., E. Swinnen, and F. Fierens (2002), GLOBSCAR Final Report, *VITO TAP/N7904/FF/FR-001 version 1.2*, Eur. Space Ag., Paris.

Lavoué, D., C. Liousse, H. Cachier, B. J. Stocks, and J. G. Goldammer (2000), Modeling of carbonaceous particles emitted by boreal and temperate wildfires at northern latitudes, *J. Geophys. Res.*, *105*(D22), 26,871–26,890.

Levine, J. S. (1996), FireSat and the global monitoring of biomass burning, in *Biomass Burning and Global Change*, edited by J. S. Levine, pp. 107–132, MIT Press, Cambridge, Mass.

Levine, J. S., W. R. Cofer III, E. L. Winstead, R. P. Rhinehart, D. R. Cahoon, D. I. Sebacher, S. Sebacher, and B. J. Stocks (1991), Biomass burning: Combustion emissions, satellite imagery, and biogenic emissions, in *Global Biomass Burning: Atmospheric, Climatic, and Biospheric Implications*, edited by J. S. Levine, pp. 264–271, MIT Press, Cambridge, Mass.

Levine, J. S., T. Bobbe, N. Ray, A. Singh, and R. G. Witt (1999), Wildland fires and the environment: A global synthesis, *Rep.UNEP/DEIAEW/TR. 99-1*, United Nations Environ. Prog., Geneva.

Liousse, C., J. E. Penner, C. Chuang, J. J. Walton, H. Eddleman, and H. Cachier (1996), A global three-dimensional model study of carbonaceous aerosols, *J. Geophys. Res.*, *101*(D14), 19,411–19,432.

Loveland, T. R., B. C. Reed, J. F. Brown, D. O. Ohlen, J. Zhu, L. Lang, and J. W. Merchant (2000), Development of a global land cover characteristics database and IGBP DISCover from 1-km AVHRR data, *Int. J. Remote Sens.*, *21*, 1303–1330.

Mack, F., J. Hoffstadt, G. Esse, and J. G. Goldammer (1996), Modeling the influence of vegetation fires on the global carbon cycle, in *Biomass Burning and Global Change*, edited by J. S. Levine, pp. 149–159, MIT Press, Cambridge, Mass.

Malingreau, J. P., and J.-M. Grégoire (1996), Developing a global vegetation fire monitoring system for global change studies: A framework, in *Biomass Burning and Global Change*, edited by J. S. Levine, pp. 14–24, MIT Press, Cambridge, Mass.

Moreno-Ruiz, J. A., P. M. Barbosa, C. Carmona-Moreno, J.-M. Grégoire, and A. S. Belward (1999), Glints-BS- global burn scar detection system, functional description and user manual document, *Publ. I. 99. 167*, Eur. Commun., Brussels.

Olivier, J. G. J., and J. J. M. Berdowski (2001), Global emission sources and sinks, in *The Climate System*, edited by J. J. M. Berdowski, R. Guicherit, and B. J. Heij, pp. 33–78, A. A. Balkema, Brookfield, Vt.

Page, S. E., F. Siegert, J. O. Rieley, H.-D. V. Boehm, A. Jaya, and S. Limin (2002), The amount of carbon released from peat and forest fires in Indonesia during 1997, *Nature*, *420*, 61–65.

Palacios, A., E. Chuvieco, and C. Carmona-Moreno (2002), Trace gas emission estimation in biomass burning: State of the art, *Publ. EUR 20376 EN*, Eur. Commun., Brussels.

Pereira, J. M. C., B. Pereira, P. Barbosa, P. D. Stroppiana, M. J. P. Vasconcelos, and J.-M. Grégoire (1999), Satellite monitoring of fire in the EXPRESSO study area during the 1996 dry season experiment: Active fires, burnt area and atmospheric emissions, *J. Geophys. Res.*, *104*(D23), 30,701–30,712.

Rahman, H., and G. Dedieu (1994), SMAC: A simplified method for the atmospheric correction of satellite measurements in the solar spectrum, *Int. J. Remote Sens.*, *15*, 123–143.

Ramankutty, N., and J. A. Foley (1998), Characterizing patterns of global land use: An analysis of global croplands data, *Global Biogeochem. Cycles*, *12*, 667–685.

Roujean, J. L., M. Leroy, and P. Y. Deschamps (1992), A bi-directional reflectance model of the Earth's surface for the correction of remotely sensed data, *J. Geophys. Res.*, *97*(D18), 20,455–20,468.

Roy, D., P. E. Lewis, and C. O. Justice (2002), Burned area mapping using multi-temporal moderate spatial resolution data—A bi-directional reflectance model-based expectation approach, *Remote Sens. Environ.*, *83*, 263–286.

San Miguel, J., A. Annoni, and G. Schmuck (1998), The use of satellite imagery for retrieval of information on wildfire damage in Mediterranean landscapes, in *Proceedings of ERIM'98, 27th International Symposium on Remote Sensing of Environment: Information for Sustainability*, pp. 758–762, ICRSE, Tromso, Norway.

Scholes, R. J., J. Kendall, and C. O. Justice (1996a), The quantity of biomass burned in southern Africa, *J. Geophys. Res.*, *101*(D19), 23,667–23,676.

Scholes, R. J., D. E. Ward, and C. O. Justice (1996b), Emissions of trace gases and aerosol particles due to vegetation burning in southern hemisphere Africa, *J. Geophys. Res.*, *101*(D19), 23,677–23,682.

Seiler, W., and P. J. Crutzen (1980), Estimates of gross and net fluxes of carbon between the biosphere and the atmosphere from biomass burning, *Clim. Change*, *2*, 207–248.

Shvidenko, A., and J. G. Goldammer (2001), Fire situation in Russia, *FAO Int. Forest Fire News*, *24*, 41–59.

Siegert, F., G. Ruecker, A. Hinrichs, and A. A. Hoffmann (2001), Increased damage from fires in logged forests during droughts caused by El Nino, *Nature*, *414*, 437–440.

Silva, J. M. N., A. M. O. Sousa, J. M. C. Pereira, K. Tansey, and J.-M. Grégoire (2002), A contribution for a global burned area map, in *Forest Fire Research and Wildland Fire Safety* [CD-ROM], edited by D. X. Viegas, Millpress, Rotterdam.

Silva, J. M. N., J. M. C. Pereira, A. Cabral, A. C. L. Sá, M. J. P. Vasconcelos, B. Mota, and J.-M. Grégoire (2003), The area burned in southern Africa during the 2000 dry season, *J. Geophys. Res.*, *108*(D13), 8498, doi:10.1029/2002JD002320.

Simon, M., S. Plummer, F. Fierens, J. J. Hoelzemann, and O. Arino (2004), Burnt area detection at global scale using ATSR-2: The GLOBSCAR products and their qualification, *J. Geophys. Res.*, *109*, doi:10.1029/2003JD003622, in press.

Stocks, B. J. (1991), The extent and impact of forest fires in northern circumpolar countries, in *Global Biomass Burning: Atmospheric, Climatic, and Biospheric Implications*, edited by J. S. Levine, pp. 197–202, MIT Press, Cambridge, Mass.

Stocks, B. J., et al. (2002), Large forest fires in Canada 1959–1997, *J. Geophys. Res.*, *107*(D24), 8149, doi:10.1029/2001JD000484 [printed *108*(D1), 2003].

Stroppiana, D., and J.-M. Grégoire (2002), Using temporal change of the land cover spectral signal to improve burnt area mapping, in *Analysis of Multitemporal Remote Sensing Images*, edited by L. Bruzzone and P. Smits, pp. 209–216, World Sci., Tokyo.

Stroppiana, D., S. Pinnock, J. M. C. Pereira, and J.-M. Grégoire (2002), Radiometric analysis of Spot Vegetation images for burnt area detection in northern Australia, *Remote Sens. Environ.*, *82*, 21–37.

Stroppiana, D., K. Tansey, J.-M. Grégoire, and J. M. C. Pereira (2003), An algorithm for mapping burnt areas in Australia using SPOT-VEGETATION data, *IEEE Trans. Geosci. Remote Sens.*, *41*, 907–909, doi:10.1109/TGRS.2003.808898.

Tansey, K. (2002), Implementation of the regional burnt area algorithms for the GBA-2000 initiative, *Publ. EUR 20532 EN*, Eur. Commun., Brussels.

Taylor, J. A., and P. R. Zimmerman (1991), Modeling trace gas emissions from biomass burning, in *Global Biomass Burning: Atmospheric, Climatic, and Biospheric Implications*, edited by J. S. Levine, pp. 345–350, MIT Press, Cambridge, Mass.

Trigg, S., and S. Flasse (2000), Characterizing the spectral-temporal response of burned savannah using in situ spectroradiometry and infrared thermometry, *Int. J. Remote Sens.*, *21*, 3161–3168.

Trigg, S., and S. Flasse (2001), An evaluation of different bi-spectral spaces for discriminating burned shrub-savannah, *Int. J. Remote Sens.*, *22*, 2641–2647.

Van Aardenne, J. A., F. J. Dentener, J. G. J. Olivier, C. G. M. Klein Goldewijk, and J. Lelieveld (2001), A $1^\circ \times 1^\circ$ resolution data set of historical anthropogenic trace gas emissions for the period 1890–1990, *Global Biogeochem. Cycles*, *15*, 909–928.

Zheng, D. L., S. D. Prince, and R. Wright (2003), NPP multi-biome: Gridded estimates for selected regions worldwide, 1989–2001, R1, http://www.daac.ornl.gov, Oak Ridge Natl. Lab., Oak Ridge, Tenn.

E. Binaghi, Università dell'Insubria, Via Ravasi 2, I-21100 Varese, Italy. (elisabetta.binaghi@uninsubria.it)

L. Boschetti, J.-M. Grégoire, and M. Maggi, European Commission Joint Research Centre, I-21027 Ispra, Italy. (luigi.boschetti@ieee.org; jean-marie.gregoire@jrc.it; marta.maggi@jrc.it)

P. A. Brivio and D. Stroppiana, Institute for Electromagnetic Sensing of the Environment, Via Bassini 15, I-20133 Milan, Italy. (brivio.pa@irea.cnr.it; dani.stroppiana@libero.it)

D. Ershov, International Forest Institute, Novocheriomushkinskaya str. 69a, 117418 Moscow, Russia. (ershov@ifi.rssi.ru)

S. Flasse, Flasse Consulting, 3 Sycamore Crescent, ME16 0AG Maidstone, UK. (stephane@flasseconsulting.net)

R. Fraser, Natural Resources Canada, Canada Center for Remote Sensing, 588 Booth St., Ottawa, ON K1A 0Y7, Canada. (robert.fraser@ccrs.nrcan.gc.ca)

D. Graetz, CSIRO Earth Observation Centre GPO 3023, Canberra, ACT 2601, Australia. (dean.graetz@eoc.csiro.au)

P. Peduzzi, United Nations Environment Programme-Early Warning Unit (UNEP/DEWA/GRID-Geneva), International Environment House, 1219 Geneva, Switzerland. (pascal.peduzzi@grid. unep.ch)

J. M. C. Pereira, Tropical Research Institute, Travessa Conde da Ribeira 9, 1300-142 Lisbon, Portugal. (jmcpereira@isa.utl.pt)

J. Silva, Department of Forestry, Technical University of Lisbon, Tapada da Ajuda, 1349-017 Lisbon, Portugal. (joaosilva@isa.utl.pt)

A. Sousa, Department of Rural Engineering, University of Évora, Apartado 94, 7002-554 Évora, Portugal. (asousa@uevora.pt)

K. Tansey, Department of Geography, University of Leicester, University Road, LE1 7RH, Leicester, UK. (kevin.tansey@le.ac.uk)